THE JOURNAL OF BIOLOGICAL CHEMISTRY VOL. 291, NO. 17, pp. 8931–8950, April 22, 2016
Published in the U.S.A.

Configuration-dependent Presentation of Multivalent IL-15: IL-15Rα Enhances the Antigen-specific T Cell Response and Anti-tumor Immunity*

Received for publication, October 20, 2015, and in revised form, December 21, 2015 Published, JBC Papers in Press, December 30, 2015, DOI 10.1074/jbc.M115.695304

Enping Hong[‡], Ilana M. Usiskin[‡], Cristina Bergamaschi[§], Douglas J. Hanlon[¶], Richard L. Edelson[¶], Sune Justesen[‖], George N. Pavlakis[§], Richard A. Flavell[**], and Tarek M. Fahmy[‡1]**

From the [‡]Department of Biomedical Engineering, Yale University, New Haven, Connecticut 06511, the Departments of [**]Immunobiology and [¶]Dermatology, Yale University School of Medicine, New Haven, Connecticut 06510, the [§]Vaccine Branch, National Cancer Institute, National Institutes of Health, Frederick, Maryland 21702, and the [‖]Department of Science, University of Copenhagen, Copenhagen 1017, Denmark

Here we report a "configuration-dependent" mechanism of action for IL-15:IL-15Rα (heterodimeric IL-15 or hetIL-15) where the manner by which IL-15:IL-15Rα molecules are presented to target cells significantly affects its function as a vaccine adjuvant. Although the cellular mechanism of IL-15 trans-presentation via IL-15Rα and its importance for IL-15 function have been described, the full effect of the IL-15:IL-15Rα configuration on responding cells is not yet known. We found that trans-presenting IL-15:IL-15Rα in a multivalent fashion on the surface of antigen-encapsulating nanoparticles enhanced the ability of nanoparticle-treated dendritic cells (DCs) to stimulate antigen-specific CD8$^+$ T cell responses. Localization of multivalent IL-15:IL-15Rα and encapsulated antigen to the same DC led to maximal T cell responses. Strikingly, DCs incubated with IL-15:IL-15Rα-coated nanoparticles displayed higher levels of functional IL-15 on the cell surface, implicating a mechanism for nanoparticle-mediated transfer of IL-15 to the DC surface. Using artificial antigen-presenting cells to highlight the effect of IL-15 configuration on DCs, we showed that artificial antigen-presenting cells presenting IL-15:IL-15Rα increased the sensitivity and magnitude of the T cell response, whereas IL-2 enhanced the T cell response only when delivered in a paracrine fashion. Therefore, the mode of cytokine presentation (configuration) is important for optimal immune responses. We tested the effect of configuration dependence in an aggressive model of murine melanoma and demonstrated significantly delayed tumor progression induced by IL-15:IL-15Rα-coated nanoparticles in comparison with monovalent IL-15:IL-15Rα. The novel mechanism of IL-15 transfer to the surface of antigen-processing DCs may explain the enhanced potency of IL-15:IL-15Rα-coated nanoparticles for antigen delivery.

It is well established that dendritic cells (DCs)[2] play a key role as professional antigen-presenting cells in initiating and coordinating antigen-specific adaptive immunity (1, 2). By constitutively sampling the external microenvironment through receptor-mediated and non-receptor mediated endocytic pathways, DCs initiate, program, and regulate the effector response against a variety of antigens (3–7). Although much is known about the immunobiology of DC antigen processing and presentation and the effect of different cytokines on DC maturation and their subsequent effect on the immune response (8), little is known about how the configuration or geometry of cytokine transmission affects the DC response. For example, physiologically, although IL-2 and IL-15 belong to the same four a-helix family of cytokines, IL-2 is transmitted as a soluble paracrine or autocrine factor (9, 10), whereas IL-15 is trans-presented on the surface of DCs and other cell types through a stable complex (11) with IL-15Rα (12, 13) or secreted as a soluble paracrine complex (14, 15). The quality and manner by which cytokines are delivered to DCs can have a profound effect on the subsequent effector immune response (16, 17).

Nanosystems such as nanoparticles (18, 19), nanotubes (20), or even macromolecular systems (21) comprise an emerging strategy for controlling antigen and cytokine transmission to DCs (22–24). Perhaps one of the most explored carriers has been the polymeric poly(lactide-co-glycolide) (PLGA) system because of its significant promise and established effect in clinical settings (25–27) and well understood methods of formulation for delivery of small-molecule drugs, nucleic acids, and protein antigens (22, 28–31). Several studies have demonstrated the promise of antigen-loaded PLGA nanoparticles as nanoparticle-based vaccines and delivery systems targeting DCs (32–39).

IL-15 is a homeostatic cytokine for CD8$^+$ T cells and natural killer cells and an important regulator of the cytotoxic immune response (40). IL-15 signals by binding to cells expressing the IL-2/IL-15 β/γ receptor and is found complexed to IL-15Rα (12–15). This IL-15:IL-15Rα complex is termed heterodimeric IL-15 (hetIL-15). IL-15Rα is expressed by several cell types in

* C. B. and G. N. P. are inventors on United States Government-owned patents and patent applications related to heterodimeric IL-15 and gene expression optimization. The content is solely the responsibility of the authors and does not necessarily represent the official views of the National Institutes of Health.

[1] To whom correspondence should be addressed: Depts. of Biomedical Engineering, Chemical and Environmental Engineering, Immunobiology, and Obstetrics and Gynecology, Yale University, 55 Prospect St., New Haven, CT 06511. Tel.: 203-432-1043; Fax: 203-432-0030; E-mail: tarek.fahmy@yale.edu.

[2] The abbreviations used are: DC, dendritic cell; PLGA, polymeric poly(lactide-co-glycolide); hetIL-15, heteromeric IL-15; APC, antigen-presenting cell; NP, nanoparticle; OVA, ovalbumin, TEM, transmission electron microscopy; aAPC, artificial antigen-presenting cell; CFSE, carboxyfluorescein succinimidyl ester.

the body, most notably by activated monocytes and DCs. Co-expression of IL-15 and IL-15Rα in the same cell and intracellular complex formation is essential for the production and function of IL-15 (11, 41, 43). IL-15Rα has a very strong affinity to IL-15 (K_D ~10^{-11} M). Indeed, the main bioactive form of IL-15 is found exclusively in a complex with IL-15Rα in humans and mice (44) and is the main form of circulating IL-15 in the blood of lymphodepleted melanoma patients (45). This mechanism of IL-15 signaling has been shown to mediate the bulk of its immunological functions, including the differentiation, activation, and survival of $CD8^+$ memory T cells and natural killer cells (46–49). IL-15 has already gained significant clinical interest as a highly promising immunotherapeutic agent (40, 50–52), and the anti-tumor efficacy of the IL-15:IL-15Rα complex has been demonstrated in a variety of preclinical tumor models (53–56).

IL-15 has also been investigated for its ability to augment antigen-specific responses stimulated by vaccines. Multiple studies using DNA vaccination models have reported that the inclusion of an IL-15 expression plasmid enhanced functional and protective immunity (57–59). The administration of the IL-15 protein as an adjuvant enhanced the antigen-specific T cell response to peptide-pulsed DCs (60) and, in a separate study, was able to increase antibody titers against a recombinant bacterial superantigen by a DC-specific mechanism (61). Some of these effects may be due to the action of IL-15 on DCs. Indeed, IL-15-transduced DCs are more activated than normal DCs and show improved survival and function (62). When given during DC differentiation, IL-15 potentiated stronger DC-mediated CD8 stimulation (63–65) and mediated reversal of the suppressive effects of the tumor microenvironment by restoring the antigen-processing machinery inhibited by tumor gangliosides (66). Therefore, IL-15 may interact with DCs and other antigen-presenting cells (APCs) to enhance their stimulation of other immune cells.

Because of the substantial ability of IL-15 to promote the activation and survival of CD8 effector and memory T cells and as a vaccine adjuvant in general, we reasoned that the inclusion of IL-15 on the surface of NPs would potentiate the response of APCs to encapsulated antigen. In previous work, our group and others have shown that the quality of antigen-specific memory $CD8^+$ T cells after immunization is increased with the sustained delivery and increased availability of antigen afforded by PLGA-mediated prolonged antigen release (33, 34, 67, 68). The humoral and cellular immune responses can be potentiated further by the introduction of rationally selected ligands to the PLGA formulation. The addition of pathogen-associated molecular patterns to antigen delivery systems, for example, generated protection against West Nile strains (33, 34), lethal avian and flu strains in mice, and H1N1 in rhesus macaques (67). The use of IL-15 as an adjuvant on nanoparticulate PLGA delivery platforms for sustained release of antigen has not yet been explored.

Here we test this potential adjuvant by binding stable complexes of IL-15:IL-15Rα to the surface of PLGA nanoparticles encapsulating the model antigen ovalbumin (OVA). IL-15:IL-15Rα presented on nanoparticles acts as an adjuvant for the DC-mediated activation of OVA-specific immune responses, and this adjuvant activity (in terms of the cellular immune response) requires the delivery of antigen and heterodimeric IL-15 to the same DCs. The adjuvant activity is mediated through transfer of IL-15 from the nanoparticles to the surface of recipient DCs through a mechanism that involved internalization of the NP and export of IL-15 to the DC membrane. Our findings reveal new strategies for the enhancement of IL-15 function *in vivo* as an immunotherapeutic adjuvant.

Experimental Procedures

Nanoparticle Formulation—Endotoxin-free OVA (InvivoGen) was encapsulated in avidin-coated PLGA nanoparticles (NPs) using a water/oil/water double emulsion technique. 2 mg of ovalbumin protein was dissolved in 200 μl of sterile PBS and added dropwise to 50 mg of PLGA (50:50 monomer ratio, Durect Corp.) dissolved in 3 ml of chloroform while vortexing. The emulsion was then added dropwise to a mixture of 3 ml of 5% poly(vinyl alcohol) and 1 ml of an avidin-palmitic acid conjugate at 5 mg/ml in 2% sodium deoxycholate while vortexing. The avidin-palmitate partitions to the chloroform-water interface, immobilizing avidin at the NP surface upon solvent evaporation (69). The double emulsion was sonicated three times for 10 s each on ice and then transferred into a 200-ml volume of 0.2% PVA in distilled H_2O to evaporate the solvent by magnetic stirring at room temperature for 90 min. Particles were then washed three times with distilled H_2O and lyophilized for long-term storage at −20 °C. The encapsulation of IL-2 or class I peptides was performed in a similar manner. 200 μg of SIINFEKL or 1 mg of MART-1_{15-40} peptide (KGHGHSYTTAEEAAGIGILTVILGVL) were dissolved in 200 μl of sterile PBS and added dropwise, while vortexing, to the PLGA/chloroform solution before emulsification in PVA as described above. For interleukin 2 (Chiron Corp.), 200 μl of a 1 mg/ml solution in PBS was used. The remaining nanoparticle formulation steps were followed after loading of the encapsulant. Nanoparticle size was analyzed using scanning electron microscopy as well as diffusion measurements in aqueous solution using a NanoSight NS500 instrument (NanoSight).

Cytokine Preparation—Optimized dual promoter plasmids expressing the two chains of the human heterodimeric cytokine IL-15:IL-15RαFc have been described previously. IL-15:IL-15RαFc is a fusion protein comprising the human soluble heterodimeric IL-15, in which the sIL-15Rα chain is fused to the Fc region of human IgG1 (70). Human IL-15:IL-15RαFc was synthesized and secreted by a stable, clonal HEK293 cell line as reported previously (15) and purified by protein A affinity chromatography. The dose of heterodimeric IL-15 in these experiments was calculated and expressed as the equivalent amount of single-chain IL-15 found within the heterodimer, as determined by amino acid analysis. The heterodimer was reacted at a 1:10 molar ratio with NHS-LC-LC-biotin (Thermo Fisher Scientific) for 1 h at 37 °C and then dialyzed for 48 h in PBS in a 3000 molecular weight cutoff dialysis bag (Thermo Fisher Scientific) to remove excess unreacted biotin.

Transmission Electron Microscopy (TEM)—IL-15-bearing NPs were treated with anti-human IL-15 (R&D Systems) and then treated with anti-mouse IgG labeled with 3-nm gold nanoparticles. The resulting NPs were mounted on copper grids,

washed, and imaged on a FEI Tecnai Biotwin TEM instrument. NP-treated cells were fixed overnight in paraformaldehyde and then sectioned under liquid nitrogen before mounting and imaging by TEM.

Preparation of Murine Antigen-specific T Cells and Bone Marrow-derived Dendritic Cells—All mice used in these studies were purchased from Taconic Biosciences. Primary splenocytes were obtained from homogenized mouse spleens. $CD8^+$ T cells were purified from the splenic homogenate of 8-16-week-old female Rag2/OT-I transgenic mice by negative immunoselection according to the instructions of the manufacturer (StemCell Technologies). T cells were cultured in complete RPMI-10 medium consisting of RPMI 1640 medium, 10% FBS, 1% L-glutamine, 50 μM β-mercaptoethanol, 1% penicillin, 1% streptomycin, 0.05% minimum essential medium vitamin solution, 1% sodium pyruvate, and 1% non-essential amino acids (all cell culture supplements were purchased from Invitrogen). When necessary, the splenic homogenate was labeled with CFSE before purification.

DCs were generated from murine bone marrow according to established protocols (72). Bone marrow was flushed out from the femora and tibiae of 8- 16-week-old C57Bl/6 mice, and erythrocytes were depleted by hypotonic lysis (Lonza). The remaining bone marrow cells were cultured in RPMI 1640 medium supplemented with 10% FBS, 1% HEPES buffer, 1% penicillin-streptomycin-glutamine, 100 μM β-mercaptoethanol, and 20 ng/ml murine GM-CSF. 5 days after the beginning of culture, non-adherent and semiadherent cells were collected and cultured in fresh medium for 2 more days before being used in experiments.

Preparation of Human Antigen-specific T Cells and HLA-$A2^+$ DCs—The human $CD8^+$ T cell receptor transgenic cell line DMF5, which is reactive to the MART-1_{27-35} epitope, was provided by John R. Wunderlich (Surgery Branch, NCI/National Institutes of Health). Protocols for generating mature monocyte-derived DCs over a 48-h period (rather than a 7- to 10-day period) have been described previously (73–75). Peripheral blood was isolated from healthy human donors (HLA-A*0201$^+$ and HLA-A*0201$^-$) after informed consent was obtained, and mononuclear cells were purified by Ficoll-Hypaque gradient centrifugation. Purified cells were suspended in serum-free DC medium (Cell-Genix) with 1% human serum and plated at 15×10^6 cells/well in a 6-well tissue culture plate. Non-adherent cells and medium were removed and replaced with fresh DC medium 90 and 150 min after the start of incubation. The media was then replaced with DC medium supplemented with 800 IU/ml GM-CSF and 1000 IU/ml IL-4 for 24 h at 37 °C to generate immature DCs capable of internalizing and cross-presenting antigen.

For stimulation with DMF-5 T cells, human DCs were first incubated with nanoparticles or other treatments overnight. A maturation mixture of 10 ng/ml TNFα, 10 ng/ml IL-1β, 1000 IU/ml IL-6, and 1 μg/ml prostaglandin E2 was added to each sample for the final 4 h of culture. DCs were then harvested, washed, and co-cultured with DMF-5 T cells at a ratio of 1:2 DCs:T cells for 72 h at 37 °C. The efficiency of antigen-specific T cell activation was assessed using a human IFN-γ ELISA kit according to the instructions of the manufacturer.

T Cell and DC Co-culture Studies—DCs were seeded in 96-well U-bottomed plates at 25,000 cells/well. Nanoparticle constructs were added to DC cultures at 0.1 mg/ml and allowed to incubate for 8 h. When necessary, avidin-coated nanoparticles were allowed to bind with biotinylated IL-15:IL-15Rα (prepared as described previously) by incubating at room temperature for 15 min. DCs were then washed twice by centrifugation at 1500 rpm for 5 min and aspirated carefully, and then the culture medium was replaced. T cells were added at 50,000 cells/well and allowed to co-incubate for 72 h. At the end of the incubation, all cells were centrifuged, and supernatants were recovered for analysis by ELISA.

Flow Cytometric Analysis—CFSE-labeled $CD8^+$ T cells were fixed in 2% paraformaldehyde and analyzed directly by flow cytometry. Before analysis, 5×10^4 6-μm polystyrene beads were added to each sample as an internal standard to determine absolute cell counts. For IL-15 retention studies, nanoparticle-treated bone marrow-derived dendritic cells were stained with phycoerythrin- or allophycocyanin-labeled anti-human IL-15 (R&D Systems) diluted 1:20 in 1% FBS in PBS. Staining was performed for 30 min at 4 °C, and then cells were washed once in 1× PBS and fixed in 2% paraformaldehyde. For detection of phosphorylated signaling molecules, cells were stimulated with IL-15 for 1 h and then fixed with 4% paraformaldehyde for 20 min. Cells were washed and then permeabilized overnight in 100% methanol at −20 °C. Finally, cells were washed and stained with Alexa Fluor 488-conjugated anti-phospho-STAT5 for 30 min at room temperature in the dark and then resuspended in 2% paraformaldehyde. All samples were run on an Accuri C6 flow cytometer (BD Biosciences), and data were analyzed using FlowJo (TreeStar) or Accuri C6 software.

Exosome Preparation—Exosomes were purified from DC culture supernatants by a sequential centrifugation protocol. DCs were incubated with NP treatments in complete medium for 24 h. DCs were then washed twice in serum-free media and replated in serum-free exosome production media containing 1% BSA for a further 24 h. Exosomes were purified from the resulting conditioned media by sequential centrifugation at 400 rcf, 2000 rcf, 10,000 rcf, and 100,000 rcf. Exosome preparations were adsorbed to 5 μm of aldehyde-sulfate beads (Life Technologies) that were then stained with antibodies and analyzed by flow cytometry.

Transwell Experiments—DCs were incubated overnight with NP constructs and then washed three times in media. 2.5×10^5 DCs/well were plated in a 24-well plate. $CD8^+$ T cells were added at a 1:1 ratio either in cell-cell contact or separated by a 400-μm pore size transwell (Costar). Cells were stimulated for 3 days and then assayed for proliferation and cytokine secretion.

Artificial APC Studies—Artificial APCs (aAPCs) were constructed by incubating avidin-coated NPs with biotin-H2-Kb MHC dimers loaded with SIINFEKL (SIINFEKL:MHC) and equimolar anti-mouse CD28 antibody (BD Biosciences). When present, biotin-IL-15:IL-15Rα was added at a concentration of 1.5 μg of IL-15/mg of NP. To compare between NP-loaded DCs and aAPCs, 0.1 mg/ml of each NP construct was used to stimulate OT-I $CD8^+$ T cells. DCs were incubated with NPs overnight and washed before adding T cells. aAPCs were added

directly to T cells. T cells were stimulated for 3 days and then analyzed for cell counts and cytokine secretion.

In Vivo Subcutaneous Tumor Studies—OVA-expressing murine B16 melanoma cells (B16-OVA) were a gift from the laboratory of Dr. Lieping Chen. B16-OVA cells were cultured in DMEM (Gibco) with 10% FBS and suspended in 1× PBS on ice prior to injection. For metastatic studies, 8-week-old C57Bl/6 mice were challenged intravenously with 1×10^5 cells injected in 50 μl of PBS. Treatments began the day after B16-OVA challenge, and mice were euthanized by CO_2 asphyxiation when symptoms of pulmonary distress were observed. Each treatment consisted of 1 μg of IL-15:IL-15Rα and 0.4 mg of PEG-modified PLGA nanoparticles.

For subcutaneous studies, 8-week-old C57Bl/6 mice were sedated with isoflurane (Baxter), and the right hind flank was shaved prior to a subcutaneous injection of 0.5×10^6 cells in 50 μl of PBS. The mice were monitored, and treatment began when the largest tumor reached 4 mm in diameter, 7–10 days after B16-OVA injection. Tumor sizes were normalized between groups after initial measurement. Systemic nanoparticle injections were performed intraperitoneally. When each component was given, each dose consisted of 1 μg of IL-15:IL-15Rα, 0.4 mg of PEG-modified PLGA nanoparticles, and 4 μg of endotoxin-free ovalbumin. Tumor size was monitored every other day by caliper measurements. Mice were euthanized by CO_2 asphyxiation when tumors reached 15 mm in greatest dimension or when the mice exhibited signs of sickness.

Results

Characterization of Antigen-loaded Nanoparticles Presenting Multivalent IL-15:IL-15Rα—Biotinylated human IL-15:IL-15Rα was mixed with avidin-coated nanoparticles at a ratio of 2 μg/ml IL-15:1 mg/ml nanoparticles. Assuming maximal binding, this ratio yields ~800 molecules of IL-15:IL-15Rα on the surface of each NP. To demonstrate complex exposure on the NP, we used phycoerythrin-labeled anti-human IL-15 and analyzed NP binding by flow cytometry. Bare nanoparticles were used as a negative control, and the dependence of IL-15:IL-15Rα on the avidin-biotin interaction was tested using nanoparticles treated with excess free biotin before binding with IL-15:IL-15Rα. Nanoparticles treated with biotinylated IL-15:IL-15Rα were stained uniformly with anti-IL-15, whereas pretreatment of nanoparticles with biotin completely inhibited IL-15 binding (Fig. 1*a*). The amount of avidin loaded onto NPs was determined by a total protein content assay to be 40 μg/mg of NP.

To qualitatively demonstrate the presence of IL-15:IL-15Rα on nanoparticles, we examined the modified NPs using TEM. Anti-human IL-15 was labeled with gold nanoparticle-linked anti-IgG1. IL-15:IL-15Rα-bound nanoparticles were labeled with gold nanoparticles, whereas gold labeling was not observed on bare nanoparticles at similar staining concentrations (Fig. 1*b*).

To show that IL-15:IL-15Rα-coated NPs were internalized by DCs, we prepared sections of DCs incubated with either IL-15:IL-15Rα-coated NPs or uncoated NPs and stained the sections for IL-15. On TEM analysis, NPs could be seen in the endosomal compartments of both DC preparations, but only

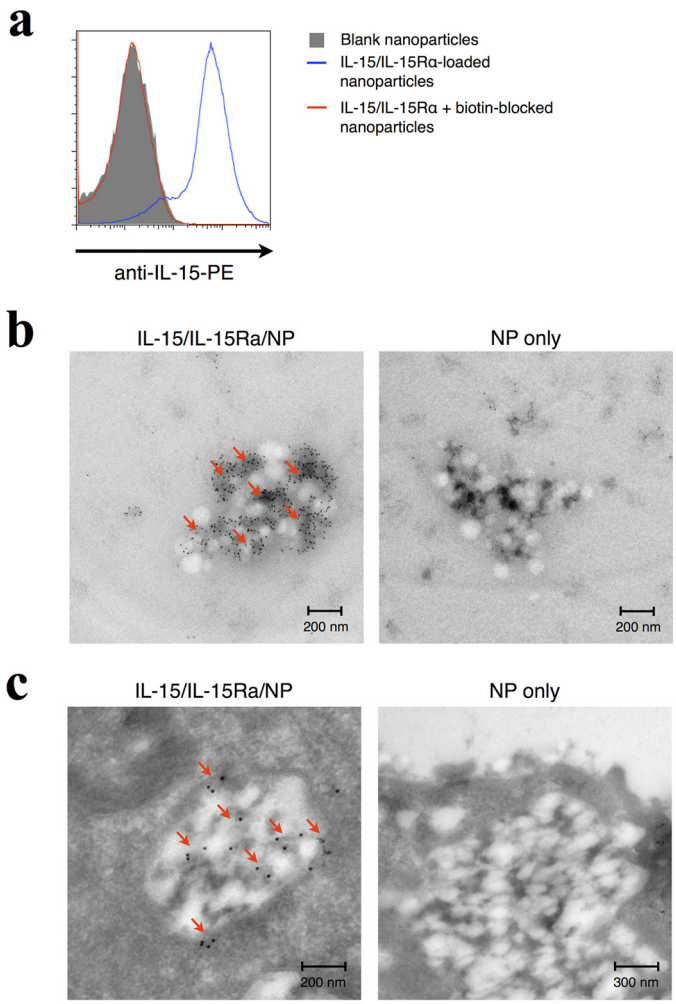

FIGURE 1. **IL-15:IL-15Rα is bound to the surface of fabricated PLGA nanoparticles.** *a*, biotinylated IL-15:IL-15Rα was incubated with avidin-coated nanoparticles to create IL-15:IL-15Rα-coated nanoparticle constructs (IL-15:IL-15Rα/NP). IL-15:IL-15Rα binding was analyzed by flow cytometry after staining with anti-human IL-15 PE. The conditions tested were IL-15:IL-15Rα/NP (*blue curve*), bare nanoparticles (*solid gray curve*), and nanoparticles blocked with excess free biotin before IL-15:IL-15Rα binding (*red curve*). *b*, TEM images of nanoparticles. IL-15:IL-15Rα/NP were stained with anti-human IL-15 and 6 nm gold-linked anti-mouse IgG1 and then imaged by TEM. *Arrows* indicate regions where gold nanoparticles are associated with IL-15 clusters on the surface of nanoparticles. *c*, TEM images of NP-treated DCs. DCs were treated with IL-15:IL-15Rα/NP or uncoated NPs and then fixed overnight in paraformaldehyde and sectioned in liquid nitrogen. Sections were stained with anti-human IL-15 and 6 nm gold-linked anti-mouse IgG1 and then imaged by TEM. *Arrows* indicate IL-15 labeling with gold nanoparticle-linked antibodies.

the IL-15:IL-15Rα-treated DCs showed IL-15 staining in the endosomal compartments (Fig. 1*c*). This confirmed that the modified NPs were internalized by DCs and that intracellular IL-15 can be detected after NP internalization.

IL-15:IL-15Rα on Nanoparticles Increases DC-mediated Stimulation of $CD8^+$ T Cells—To assess the effect of IL-15:IL-15Rα NP (without encapsulated antigen) on DC-mediated stimulation of $CD8^+$ T cells, NPs with and without the IL-15 complex were first incubated with murine bone marrow-derived DCs. Because human IL-15:IL-15Rα is cross-reactive with both mouse and human cells (15, 44), it is suitable for use in our murine experimental system. CD8 responses were monitored using purified splenic $CD8^+$ T cells from OT-I transgenic mice

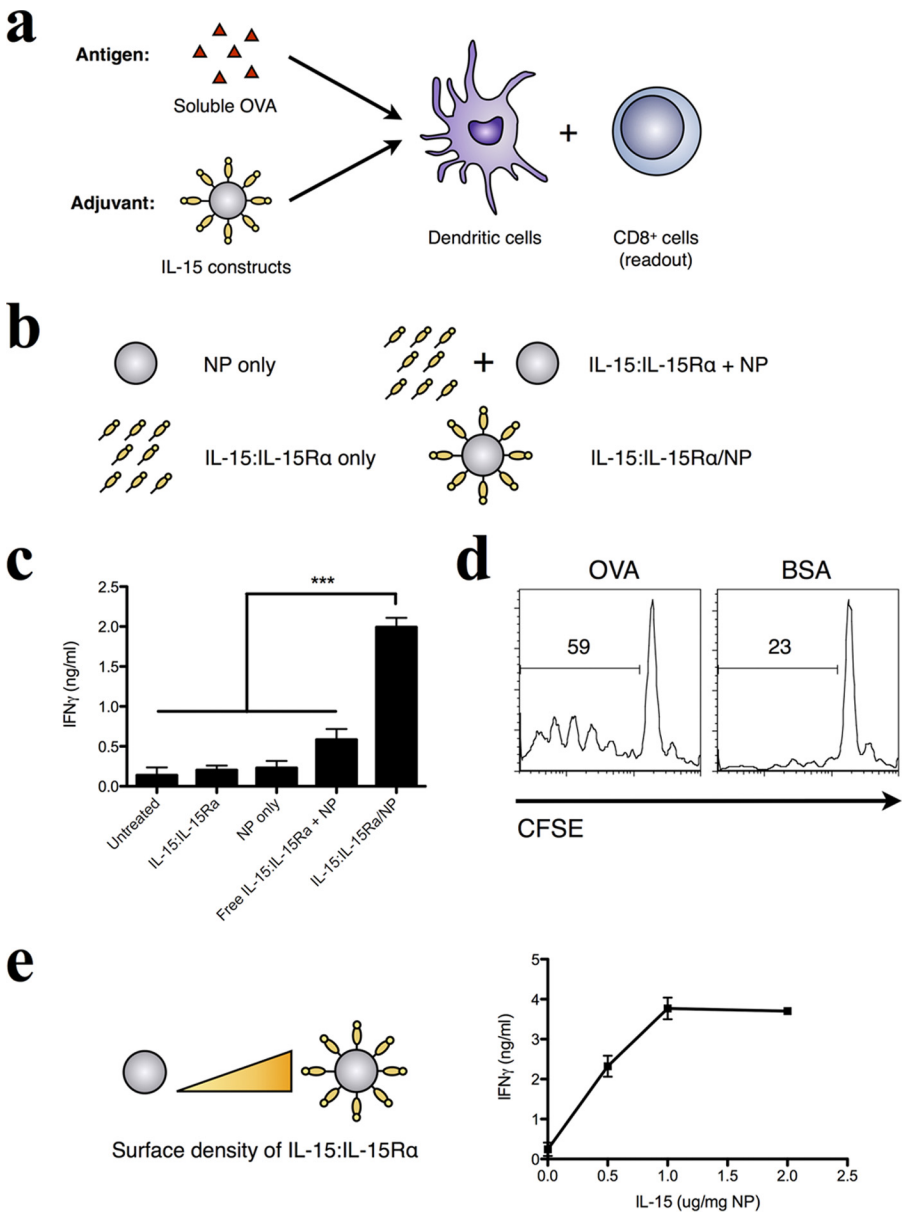

FIGURE 2. **IL-15:IL-15Rα-bearing nanoparticles stimulate cross-priming of antigen-specific CD8$^+$ T cells by DCs.** *a*, DCs were incubated with 50 μg/ml of soluble endotoxin-free OVA for 8 h and then washed and co-incubated with purified OVA-specific CD8$^+$ T cells. 72 h later, cytokine levels in cell culture supernatants were evaluated by ELISA. *b*, during antigen uptake, DCs were co-incubated with various adjuvant formulations as depicted. Avidin-coated PLGA nanoparticles were given at 0.1 mg/ml, and IL-15:IL-15Rα was given at 0.2 μg/ml. Biotinylated IL-15:IL-15Rα was loaded onto nanoparticles by mixing the components for 15 min at room temperature before adding to DCs. For conditions where IL-15 is separated from the nanoparticle surface (*IL-15:IL-15Rα + NP*), nanoparticles were blocked with free biotin for 15 min before addition of IL-15. *c*, the adjuvant effect of these formulations was evaluated by IFN-γ production from OT-I CD8$^+$ T cells. Data were analyzed by a one-way ANOVA and a Tukey post-hoc test. *** indicates a significance level of $p \leq 0.001$. *d*, the antigen-specific nature of the T cell response was tested in the case of a specific antigen (OVA) and nonspecific antigen (BSA) using CFSE-labeled OT-I CD8$^+$ T cells as responder cells. *e*, IL-15 was titrated on a fixed concentration of nanoparticles to determine the dose dependence of IFN-γ production on IL-15 concentration. These results are representative examples of multiple ($n = 3$) identical experiments.

specific for the K^b-restricted peptide SIINFEKL (OVA 257–264) (76). DCs were incubated with 50 μg/ml exogenous OVA in the presence of various IL-15:IL-15Rα-bearing nanoparticle constructs (Fig. 2*a*). Additionally, we compared the effect of free IL-15:IL-15Rα together with free antigen. To control for effects induced by the nanoparticle vehicle itself, two additional controls were included: nanoparticles alone and nanoparticles preincubated with biotin to block surface binding sites and then mixed with IL-15:IL-15Rα (Fig. 2*b*).

When DCs were incubated with soluble OVA and nanoparticles bearing IL-15:IL-15Rα, a greater production of IFN-γ was observed compared with free IL-15:IL-15Rα at identical concentrations (Fig. 2*c*). In the absence of CD8$^+$ T cells, little IFN-γ was observed (data not shown), implicating CD8$^+$ T cells as the major producer of observed IFN-γ upon DC stimulation. The activation of CD8 T cells was antigen-specific because OT-I T cells failed to proliferate when an equal concentration of exogenous BSA was used in place of OVA (Fig. 2*d*). Interestingly, increasing the density of surface-bound IL-15:IL-15Rα correlated with increased levels of IFN-γ produced by CD8$^+$ T cells, suggesting a dose-response effect on IFN-γ because of IL-15:IL-15Rα treatment (Fig. 2*e*). These results indicate that nanopar-

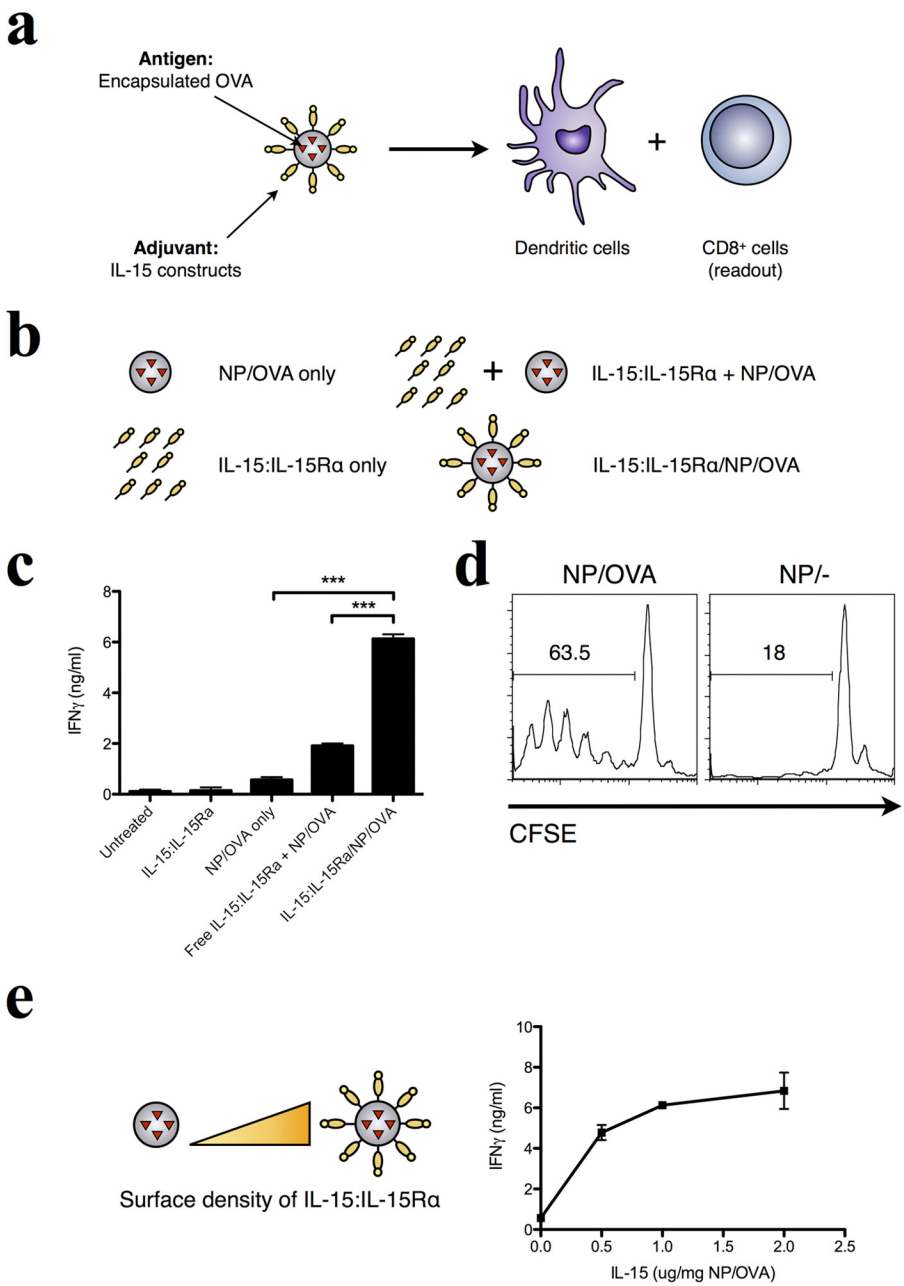

FIGURE 3. **Surface-presented IL-15:IL-15Rα enhances the immunostimulatory capacity of antigen-loaded nanoparticles for the DC-mediated cross-priming of CD8$^+$ T cells.** *a*, the adjuvant nature of IL-15:IL-15Rα was confirmed in assays where endotoxin-free OVA was encapsulated within nanoparticles at 40 μg of OVA/mg of NP. *b*, the same adjuvant constructs were tested as in Fig. 1. *c*, the adjuvant effect of these formulations was evaluated by IFN-γ production from OT-I CD8$^+$ T cells. Data were analyzed by a one-way ANOVA and a Tukey post-hoc test. *** indicates a significance level of $p \leq 0.001$. *d*, the antigen-specific nature of the T cell response was tested with nanoparticles encapsulating OVA (*NP/OVA*) and unloaded nanoparticles (*NP/*−) using CFSE-labeled OT-I CD8$^+$ T cells as responder cells. *e*, IL-15 was titrated on a fixed concentration of OVA-loaded nanoparticles to determine the dose dependence of IFN-γ production on IL-15 concentration.

ticles presenting IL-15:IL-15Rα act to enhance the antigen-specific cross-priming of CD8$^+$ T cells by DCs.

Previous work has shown that the rate of antigen delivery (persistence of antigen) affects the long-term memory immune response and vaccine efficacy in pathogen recall (67, 68). We therefore hypothesized that multivalent presentation of IL-15:IL-15Rα may synergize with antigen encapsulation in PLGA to enhance CD8$^+$ T cell stimulation (Fig. 3*a*). PLGA nanoparticles encapsulating ovalbumin (NP/OVA) were prepared by a double emulsion method and used as the antigen source in place of exogenous OVA (Fig. 3*b*). NP/OVA particles were determined to have loaded 40 μg of OVA/mg of NP. When IL-15:IL-15Rα was trans-presented on nanoparticles that also encapsulated antigen, CD8$^+$ T cell activation by DCs that internalized these particles was similarly enhanced above that of free IL-15:IL-15Rα alone, NP/OVA alone, or NP/OVA with IL-15:IL-15Rα separated from the particle surface (Fig. 3*c*). As before, when T cells were removed, cytokine production was abrogated (data not shown). The antigen specificity of the CD8$^+$ response was confirmed when particles without antigen loading failed to elicit T cell proliferation (Fig. 3*d*). In addition, the IFN-γ response was dependent on IL-15:IL-15Rα surface density on

the antigen-loaded nanoparticles (Fig. 3*e*), similar to what was observed with exogenous antigen. The resulting maximal IFN-γ responses in this experiment were much higher than those shown in Fig. 2 (6 ng/ml in Fig. 3*c versus* 2 ng/ml in Fig. 2*c*), indicating a stronger immune response elicited by the encapsulated antigen (38, 39, 77, 78). We confirmed this by comparing free OVA and NP/OVA particles at the same dose (data not shown).

Taken together, these results demonstrate that the surface presentation of IL-15:IL-15Rα on nanoparticles enhances the capacity of DCs to cross-prime $CD8^+$ T cells in an antigen-specific manner. This effect was confirmed in cases where antigen was either internalized exogenously (Fig. 2) or present within the signaling nanoparticles (Fig. 3). We also verified that the DC-T cell interaction is critical for the cytokine response because the exposure of either cell type alone to IL-15:IL-15Rα nanoparticle constructs failed to produce significant levels of cytokines (data not shown). We therefore conclude that IL-15:IL-15Rα is able to act within the context of the DC:T cell interface to enhance the DC-mediated T cell response.

Synergy between Heterodimeric IL-15 and Encapsulated Antigen Requires Coordinated Delivery to DCs and T Cells—The antigen delivery system employed here has two components: IL-15:IL-15Rα trans-presented on NPs, which we have shown to be more effective than free IL-15:IL-15Rα in inducing $CD8^+$ T cell responses, and encapsulated antigen (OVA), which is also more effective than free antigen for cross-presentation and induction of both $CD4^+$ and $CD8^+$ T cell responses (33, 39, 77). Given their separate functions, we asked whether the co-localization of both multivalent IL-15 and encapsulated antigen offer clear advantages compared with separate NPs delivering both elements. It is currently unknown whether the co-localized delivery of multivalent IL-15 and antigen to antigen-presenting cells has an effect on the effector response. We tested this hypothesis in three different ways, comparing our results each time to NPs presenting the IL-15 heterodimer and encapsulating OVA antigen (IL-15/NP/OVA, *black columns* to the right of each plot in Fig. 4).

First, we hypothesized that the delivery of multivalent IL-15 (IL-15-NP) and encapsulated OVA (NP/OVA) to the same cells would be more effective than if they were delivered to separate cells. DCs were incubated with empty IL-15:IL-15Rα-coated NPs (IL-15/NP-DCs). Separately, another population of DCs from the same batch were incubated with OVA-encapsulating NPs (NP/OVA-DCs). These cells were mixed together at a ratio equivalent to the ratio of IL-15:IL-15Rα and antigen associated with a single particle (IL-15/NP-DC + NP/OVA-DC). DCs incubated with separate or single particles (maintaining the same ratio of IL-15 to antigen) were then used to stimulate OT-I $CD8^+$ T cells. We found that mixed cells (separately receiving either IL-15 or antigen) were less effective at inducing CD8 T cell proliferation than the combined particle system (IL-15/NP/OVA) (Fig. 4*a*). Notably, the mixed DCs produced IFN-γ responses on par with IL-15/NP-DCs and NP/OVA-DCs, suggesting that enhanced $CD8^+$ T cell responses are stimulated by the localization and potential synergy of IL-15 and antigen at the same DC.

IL-15 can powerfully affect $CD8^+$ T cell proliferation and activation and also enhance their persistence *in vivo* (17, 48, 79, 80). Indeed, tumor or virus-specific T cells cultivated with IL-15 have been shown to exhibit a high activity against their respective antigenic targets (81). Therefore, we hypothesized that NP-presented IL-15:IL-15Rα may also prime $CD8^+$ T cells against NP/OVA-loaded DCs. To address this question, we incubated OT-I $CD8^+$ T cells overnight with buffered saline as a control (T), IL-15:IL-15Rα alone (15-T), or nanoparticle-bound IL-15:IL-15Rα (15NP-T). We separately stimulated DCs with antigen by loading them with NP/OVA particles (Fig. 4*b*, *left panel*). After 12 h, T cells and DCs were washed, counted, plated together at the appropriate cell concentrations, and allowed to incubate for a further 72 h. The results are shown in Fig. 4*b*. We observed that $CD8^+$ T cell proliferation in response to antigen-loaded DC was greater when T cells were preincubated with IL-15:IL-15Rα. Interestingly, NP-bound IL-15:IL-15Rα was a stronger priming stimulus compared with free IL-15:IL-15Rα (Fig. 4*b*, *right panel*). In addition, the proliferation of $CD8^+$ T cells preactivated with IL-15:IL-15Rα/NP and incubated with NP/OVA-DCs (Fig. 4*b*, *NP/OVA-DC + 15NP-T*) was greater compared with the one obtained with DCs using the combined nanoparticle platform (Fig. 4*b*, *IL-15/NP/OVA*, *black column*). This result suggested that IL-15 trans-presented on NP and antigen-loaded NP may function on the separate axes of effector cells and antigen-presenting cells. IL-15 may act to prime and activate CD8s to respond to antigen, whereas nanoparticle-encapsulated antigen is internalized by DCs and cross-presented to CD8s.

Having tested how our nanoparticle components work when delivered to different cells (separate delivery to different DCs and separate delivery to $CD8^+$ cells and DCs), we then tested a case where all nanoparticle components were delivered to the same DC. We asked whether the IL-15 and antigen components had to be presented on the same NP vehicle or whether trans-presented IL-15 and encapsulated antigen could still synergize when delivered on separate NP vehicles. We made separate nanoparticle constructs with trans-presented IL-15:IL-15Rα and encapsulated antigen, respectively, and prevented transfer of any biotinylated IL-15:IL-15Rα by blocking the avidin binding sites on NP/OVA using free biotin. We then tested these separated constructs (IL-15:IL-15Rα/NP + NP/OVA) alongside the combined construct (IL-15:IL-15Rα/NP/OVA) and along with the separate components in soluble form. We found that the combined construct was the most effective at stimulating $CD8^+$ T cell proliferation (Fig. 4*c*), indicating that delivery on the same vehicle is needed for maximal stimulation. Again, both the separate and combined constructs performed significantly better than the soluble configurations where IL-15 and OVA were delivered apart from their optimal NP configurations (Figs. 2 and 3). Overall, these results demonstrate a need for the localized delivery of trans-presented IL-15:IL-15Rα and encapsulated antigen for synergy to occur.

Multivalent IL-15:IL-15Rα on NP Functions in the Same Manner with Human Cells—The translational potential of these findings depends on whether the same findings are observed with human effector and antigen-presenting cells. To

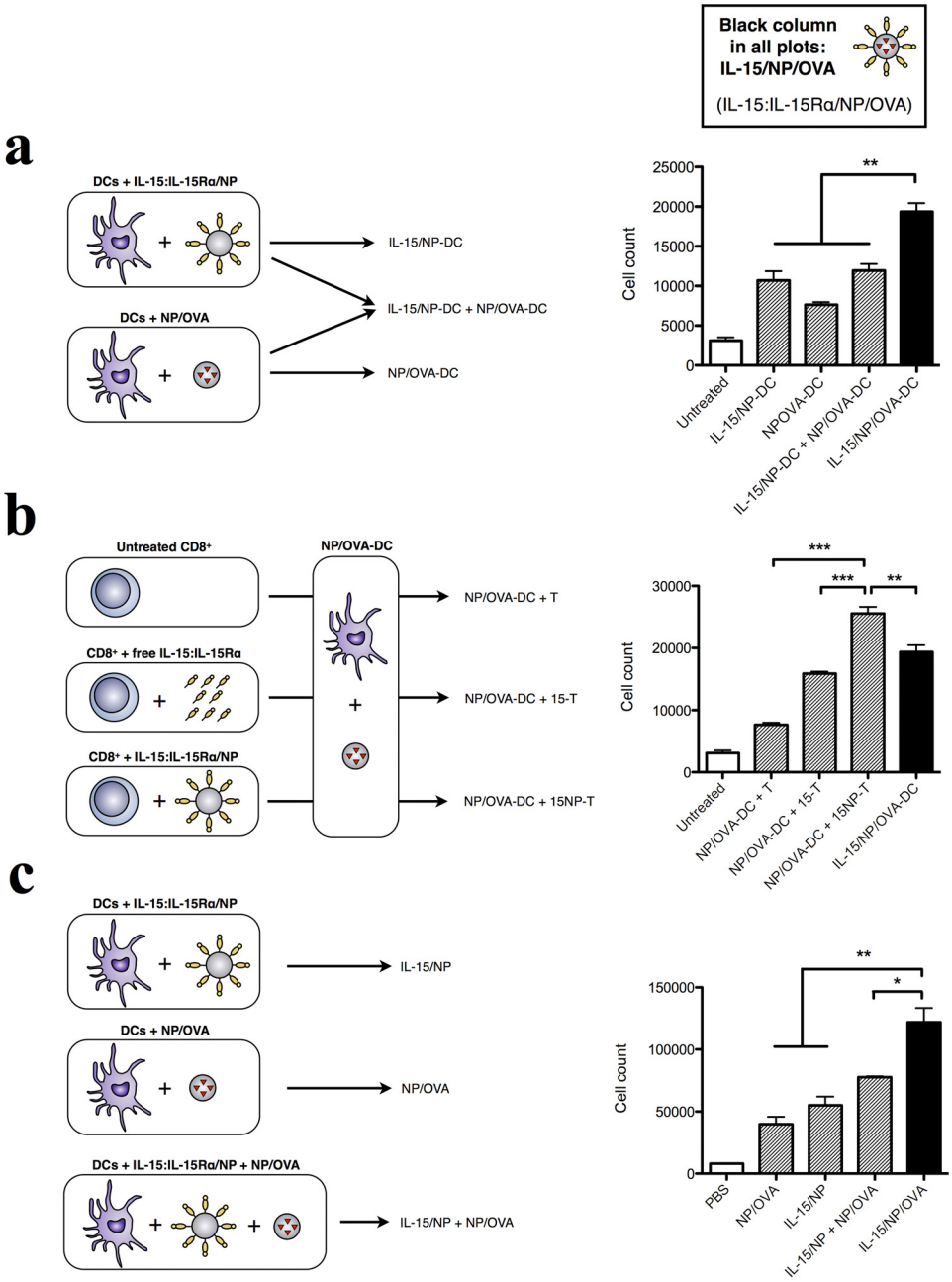

FIGURE 4. **The effects of trans-presented IL-15:IL-15Rα and encapsulated antigen require coordinated delivery to DCs and T cells.** To investigate the requirements for the adjuvant effect of IL-15:IL-15Rα, DCs were compared in their ability to stimulate OT-I CD8$^+$ T cells under different conditions of IL-15:IL-15Rα and OVA delivery. *a*, the requirement for both particle types to go to the same cell was tested by mixing DCs that were separately given IL-15/NP or NP/OVA and comparing them with DCs given IL-15/NP/OVA. *b*, the effect of priming CD8+ T cells with IL-15 constructs was tested by priming CD8$^+$ T cells overnight with free or NP-bound IL-15:IL-15Rα and stimulated with NP/OVA-DCs. *c*, to test the requirement for OVA or IL-15 to be delivered on the same particle, DCs were incubated with different particle constructs overnight and then used to activate OT-I CD8$^+$ T cells. In all cases, the T cell response was compared against untreated DCs and IL-15/NP/OVA-treated DCs. OT-1 cell counts were determined as a measure of total stimulatory capacity of each group. Data were analyzed by a one-way ANOVA and a Tukey post-hoc test. * indicates a significance level of $p \leq 0.05$, ** $p \leq 0.01$, and *** indicates $p \leq 0.001$.

validate our findings using a clinically relevant human antigen, NPs were loaded with a 26-mer peptide derived from the Melan-A/MART-1 melanoma-specific antigen (82). IL-15:IL-15Rα NPs loaded with the MART-1 antigen were incubated with human HLA-A2$^+$ DCs and then used to stimulate DMF-5 responder cells (Fig. 5*a*). DMF-5 cells carry TCR receptors specific for the MART-1_{27-35} sequence and respond to antigen-specific stimulation by producing IFN-γ (83). Consistent with observed findings in the mouse system with the encapsulated OVA antigen, the MART-1 antigen encapsulated in NPs trans-presenting multivalent IL-15:IL-15Rα led to a greater IFN-γ response from DMF5 cells compared with soluble IL-15:IL-15Rα (Fig. 5*b*). This result highlights the clinical potential of this mode of IL-15 delivery and possibly points to the promise of enhancing a cytokine response by changes in the contextual delivery aspect compared with, for example, genetic manipulation of the IL-15 protein sequence to affect the desired response (84, 85).

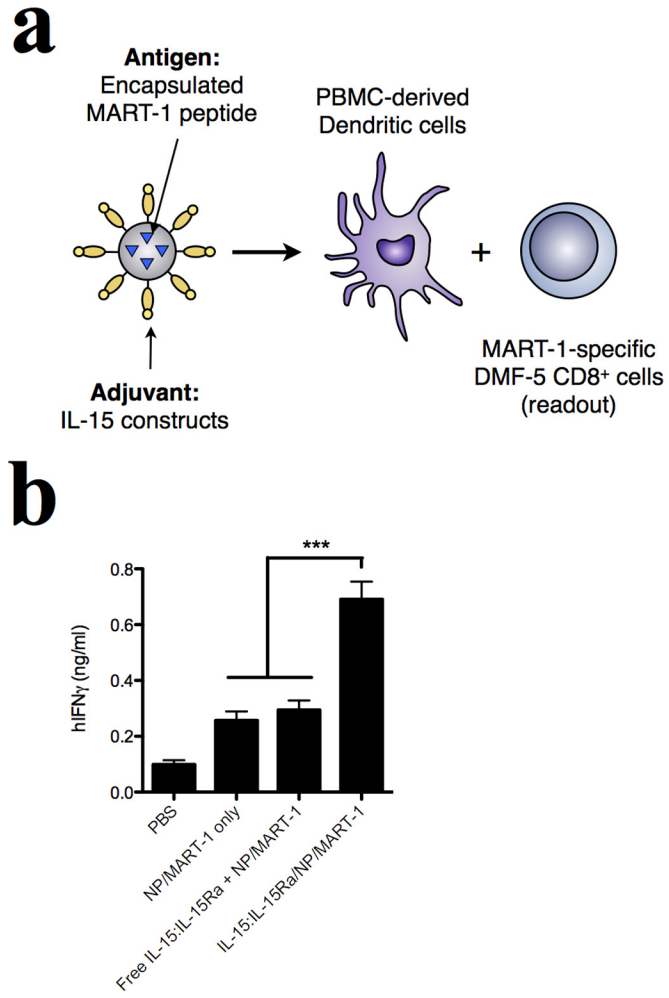

FIGURE 5. **IL-15:IL-15Rα-bearing nanoparticles stimulate cross-priming of human antigen-specific CD8$^+$ T cells by DCs.** *a*, nanoparticles encapsulating a MART-1-derived 26-mer peptide were loaded into human HLA-A2$^+$ PBMC-derived DCs and used to stimulate MART-1-specific DMF-5 T cells. *b*, the adjuvant effect of the nanoparticle formulations was evaluated by IFN-γ production from DMF-5 cells after 72 h in culture with DCs. Data were analyzed by a one-way ANOVA and a Tukey post-hoc test. *** indicates a significance level of $p \leq 0.001$. *PBMC*, peripheral blood-derived mononuclear cells.

The Mechanism of Action of Multivalent NP-presented IL-15:IL-15Rα Involves Particle-mediated Transfer of IL-15 to the DC Surface—We set out to determine the molecular mechanism by which IL-15:IL-15Rα augments the stimulatory capacity of antigen-presenting DCs. Because IL-15 trans-presentation on DCs affects the activation of CD8 T cells, we asked whether delivered IL-15 may be retained on the surface of DCs for stimulation during T cell encounters. To address this question, we treated mouse DCs with free human IL-15:IL-15Rα, nanoparticle-bound IL-15:IL-15Rα, or IL-15:IL-15Rα mixed with biotin-blocked nanoparticles and stained DCs for human IL-15 2 h later. Staining for human IL-15 ensured that we would detect only the delivered molecules and not endogenous murine IL-15. We found that incubating DCs with nanoparticle-bound IL-15:IL-15Rα resulted in increased levels of detectable human IL-15 on the DC surface in a manner commensurate with the density of IL-15:IL-15Rα on the nanoparticle surface. In contrast, free human IL-15:IL-15Rα did not result in accumulation of human IL-15 on the DC surface (Fig. 6*a*).

We next sought to characterize the persistence of this IL-15:IL-15Rα retention on the DC surface. DCs were treated with IL-15:IL-15Rα constructs for 2 h, washed, and cultured over time before staining with phycoerythrin-labeled anti-human IL-15. DCs treated with NP-bound IL-15:IL-15Rα showed an initial 200% increase in fluorescence because of IL-15 labeling compared with untreated controls (Fig. 6*b*). Although the fluorescence decayed steadily over 8 h, a strikingly high level of IL-15 was still retained on the surface of DCs, leading to a >100% increase in IL-15:IL-15Rα-associated fluorescence compared with untreated cells. This amount was steady after 8 h and remained despite wash steps. In contrast, when IL-15:IL-15Rα was given in soluble form, very little IL-15 accumulated at the DC surface, and what little did accumulate was cleared quickly from the membrane (Fig. 6*b*).

Next we asked whether the surface-retained IL-15:IL-15Rα was able to functionally stimulate CD8$^+$ T cells. DCs were treated with different concentrations of nanoparticle-bound IL-15:IL-15Rα for 2 h, resulting in different levels of IL-15 retention on the DC surface, as revealed by flow cytometry. DCs were then washed and used to stimulate purified CD8$^+$ T cells at a 1:1 DC:T cell ratio for 1 h. T cells were then stained for phosphorylated STAT5 to evaluate IL-15-specific signaling. We found that increasing levels of IL-15 on the DC surface correspondingly increased the level of phosphorylated STAT5 in CD8$^+$ T cells (Fig. 6*c*), demonstrating that the IL-15 delivered to the surface of DCs remains functional and capable of stimulating CD8$^+$ T cells.

Because IL-15 is present in high concentrations at the DC surface within a short time after NP delivery, it is possible that non-internalized NP nonspecifically associated with the cell membrane and displayed IL-15, leading to the observed high IL-15 levels at steady state. If this is the case, then the treatment of DCs with avidin-coated NPs (the base scaffold on which IL-15 is displayed) would result in the display of avidin binding sites on the DC surface, allowing for the binding of biotinylated ligands such as biotin-IL-15:IL-15Rα. To test this hypothesis, DCs were incubated with avidin-coated NPs in either media or PBS for 1 h at 37 °C. Biotin-IL-15:IL-15Rα was then added to the DCs for 15 min (Fig. 6*d*; *NP, then IL-15:IL-15Rα*; *red line*). All cells were washed and stained for IL-15 and analyzed by flow cytometry.

When the experiment was performed in media, avidin binding sites could not be detected via IL-15-associated fluorescence (Fig. 6*d*, *left panel*). However, when the experiment was performed in PBS, the "NP, then IL-15:IL-15Rα" group resulted in fluorescence similar to our positive control (Fig. 6*d*, *IL-15:IL-15Rα/NP, blue line*), suggesting the binding and detection of IL-15 at the DC surface (Fig. 6*d*, *right panel*). Biotin blockade prior to IL-15 binding (Fig. 6*d*; *NP, biotin block, then IL-15:IL-15Rα, green line*) abrogated the IL-15 signal, showing that the effect is due to biotin binding sites on the cell surface. IL-15 labeling was not detected after treating the cells with free IL-15:IL-15Rα alone, indicating that this effect is not due to any biotin binding proteins on the cell surface (Fig. 6*d*).

If IL-15-bearing NPs associate nonspecifically with the DC surface, then DCs may be able to retain IL-15 at their membranes in the absence of active cell processes. We therefore

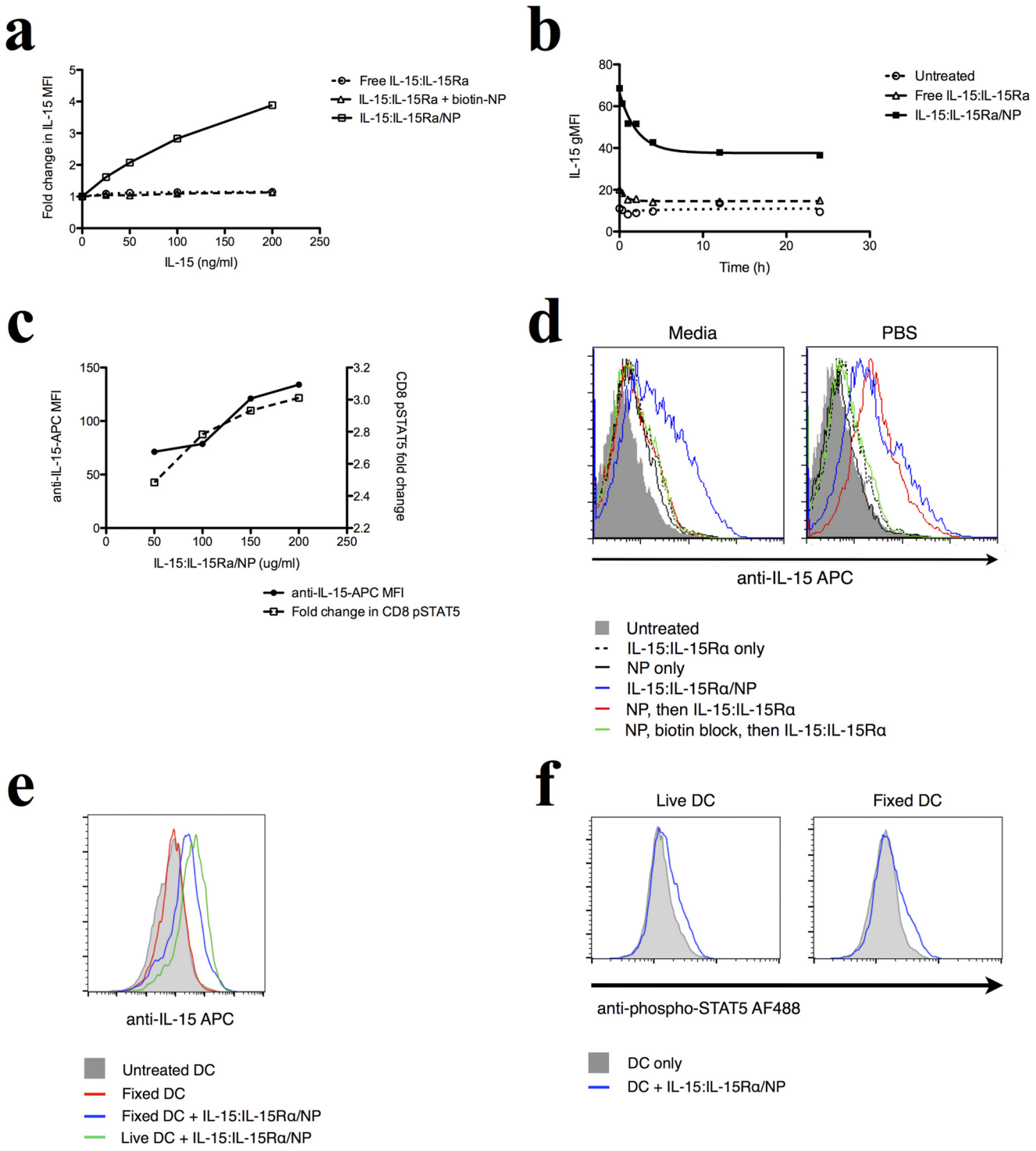

FIGURE 6. **Delivered NP-bound IL-15 is retained on the surface of DCs and signals CD8$^+$ T cells.** *a*, DCs were incubated with different concentrations of free or NP-bound IL-15:IL-15Rα constructs for 2 h and then stained for human IL-15. *b*, to track the fate of surface-retained IL-15 on DCs over time, DCs were incubated with 150 ng/ml of free or NP-bound IL-15 for varying amounts of time and then fixed and stained for human IL-15. *c*, DCs were incubated with different levels of IL-15:IL-15Rα-bound nanoparticles for 1 h and then washed and incubated with purified CD8 T cells for 1 h. CD8 cells were fixed and stained for phosphorylated STAT5. *d*, to determine whether avidin binding sites are detectable on the surface of NP-treated cells, DCs were incubated with NPs in PBS for 1 h and then exposed to biotinylated IL-15. IL-15/NP was given as a positive control, and some cells were blocked with biotin after NP binding to saturate avidin binding sites. This experiment was performed in both media and PBS. *e*, fixed and live DCs were co-incubated with IL-15-coated NPs for 2 h and then washed extensively and used to stimulate purified CD8$^+$ T cells. T cells were then stained for phospho-STAT5. Curves where IL-15 was present are shown in *blue*, and control cells are shown in *gray*. *f*, fixed and live DCs were co-incubated with IL-15-coated NPs for 2 h and then washed and stained for IL-15.

investigated the ability of fixed DCs to present IL-15 to CD8$^+$ T cells. DCs were fixed with paraformaldehyde and then incubated with IL-15:IL-15Rα/NP for 2 h. We found that these fixed, IL-15-treated DCs stained positive for IL-15, indicating that fixed DCs can accumulate IL-15 on their surface (Fig. 6*e*). The IL-15 staining was at a lower level

than live DCs (Fig. 6*e*, *green line*) exposed to IL-15:IL-15Rα/NP for the same duration, indicating that some active cellular mechanisms may aid in (but are not required for) IL-15 accumulation on the cell surface.

Finally, we asked whether the IL-15 presented on the surface of fixed DCs was bioactive. Live and fixed DCs were co-incubated with IL-15:IL-15Rα/NP for 2 h and then washed extensively and incubated with $CD8^+$ T cells for 1 h. Phospho-STAT5 staining was used to assess IL-15 signaling in $CD8^+$ cells, and live or fixed DCs unexposed to IL-15 were used as controls. We found that the IL-15 present on the surface of both live and fixed DCs was able to stimulate STAT5 phosphorylation in $CD8^+$ T cells (Fig. 6*f*), demonstrating that fixed DCs are able to present bioactive IL-15.

Our data suggest that the incubation of DCs with NPs results in some of the NPs embedding in the cell surface, exposing their surface ligands (IL-15 or avidin) for interactions with neighboring cells. Such behavior could account for the retention of IL-15 on the DC surface. The fact that IL-15 binding (in the NP, then IL-15:IL-15Rα group) could not be detected in the presence of media suggests that media components were able to shield or block the interaction of biotin-IL-15 with embedded avidin-NPs. Indeed, under the right circumstances, the avidin-biotin interaction on a surface can be blocked or inhibited (86, 87). Furthermore, active cellular mechanisms are not required for the retention of bioactive IL-15 at the DC surface. Although fixed DCs cannot process and present antigen, they are able to act as physical scaffolds for NP-delivered multivalent IL-15. Overall, our findings demonstrate that nanoparticle-bound IL-15:IL-15Rα delivers functional IL-15:IL-15Rα to the surface of DCs in a manner dependent on the density of IL-15:IL-15Rα bound to the nanoparticles and persists on the DC surface for at least 24 h.

NP-delivered IL-15 Is Not Observed on DC-derived Exosomes—We investigated the possibility that IL-15 might be exported from the DC membrane via exosomes. Indeed, IL-15Rα has been detected previously on human DC-derived exosomes (88). We therefore purified exosomes from DCs by sequential ultracentrifugation (89). DCs were allowed to take up NPs overnight (untreated control, free IL-15:IL-15Rα, NP only, and IL-15:IL-15Rα/NP), and then exosomes were purified from the DC-conditioned media. Exosome preparations were examined by TEM, revealing circular and cup-shaped membrane vesicles about 100 nm in diameter (Fig. 7*a*). Exosome size distribution was also determined by particle tracking analysis (NanoSight) and found to be between 100 and 300 nm (Fig. 7*b*).

We then examined exosome-associated proteins in our preparations by flow cytometry. All exosome preparations stained positive for class II MHC and slightly positive for CD86 (Fig. 7*c*), both of which are known to be present in DC-derived exosomes (90). However, none of the exosome preparations contained detectable levels of IL-15 (Fig. 7*c*), suggesting that IL-15 is not associated with DC-derived exosomes.

If IL-15 and antigen were being rereleased by exosomes, then DC-derived exosomes may be able to directly stimulate OT-I T cells in the absence of cell contact. We therefore tested the ability of our NP-treated DCs to stimulate T cell activation in a transwell experiment. DCs were incubated overnight with the following nanoparticle constructs: IL-15:IL-15Rα/NP, NP/OVA, and IL-15:IL-15Rα/NP/OVA. After extensive washing to remove excess NPs, DCs were used to stimulate $CD8^+$ T cells either in cell-cell contact or separated by a 400-μm pore size transwell. The addition of the transwell completely abolished the proliferative (Fig. 7*d*, *left panel*) and cytokine response (Fig. 7*d*, *right panel*) of the $CD8^+$ T cells for all NP groups, suggesting that exosomes do not carry IL-15 or antigen to T cells across the transwell membrane. We therefore conclude that IL-15 is not observed on DC-derived exosomes and that it does not contribute to T cell stimulation via an exosome-mediated mechanism.

IL-15 Enhancement of the Antigen-specific $CD8^+$ Response Mediated by NP Multivalent Presentation Is Not due to Enhancement of Antigen Processing, NP Uptake, or DC-specific IL-15 Signaling—Given that NP delivered an encapsulated form of the whole OVA protein, we next asked whether IL-15:IL-15Rα was acting on the antigen-processing machinery in DCs. To answer this question, we encapsulated the SIINFEKL peptide within IL-15:IL-15Rα-coated nanoparticles. We observed that a stronger IFN-γ response was obtained than when either IL-15:IL-15Rα was not added or detached from the biotin-blocked nanoparticle surface (Fig. 8*a*). APCs incubated with IL-15:IL-15Rα NP therefore potentiate $CD8^+$ T cell stimulation in a manner independent of antigen.

Next we asked whether NP-presented IL-15:IL-15Rα affected the rate of NP internalization and, therefore, antigen uptake. Avidin-coated NPs were surface-labeled with Alexa Fluor 488 and then incubated with DCs in the presence or absence of surface-bound IL-15:IL-15Rα. DCs were fixed and analyzed for Alexa Fluor 488 fluorescence by flow cytometry. We found that IL-15:IL-15Rα had no discernable effect on the rate of fluorescence accumulation in DCs (Fig. 8*b*), indicating that the trans-presentation of IL-15:IL-15Rα does not affect the rate of NP internalization in our system.

Finally, we asked whether IL-15:IL-15Rα induces its effects by activating signaling pathways within DCs during NP uptake. 2 h prior to NP uptake, DCs were incubated with either 10 μg/ml anti-human IL-15, 50 μM STAT5 inhibitor (*N*′-((4-oxo-4H-chromen-3-yl)methyl-ene)nicotinohydrazide), 2 μM PI3K inhibitor (LY294002), or 2 μM MEK inhibitor (U0126). We assessed the effect of these inhibitors by evaluating the -fold increase in CD8-mediated IFN-γ secretion when surface-bound IL-15:IL-15Rα was added to NP/OVA during particle uptake by DCs. Although the addition of anti-human IL-15 did partially decrease IFN-γ production, none of the other inhibitors appreciably affected the activation of $CD8^+$ T cells by the NP-loaded DCs (Fig. 8*c*). In addition, DCs did not show elevated levels of STAT5 phosphorylation upon stimulation with IL-15:IL-15Rα, lending support to our hypothesis that the primary effect of delivered IL-15:IL-15Rα to DCs is to stimulate neighboring T cells.

Artificial Antigen Presentation Together with IL-15:IL-15Rα Improves the Sensitivity and Magnitude of the Antigen-specific Response—APCs provide at least three essential signals to activate T cells: antigen-specific stimulation by peptide-MHC complexes; costimulatory signals, most commonly via the CD28/B7 interaction; and the release of cytokines to modulate

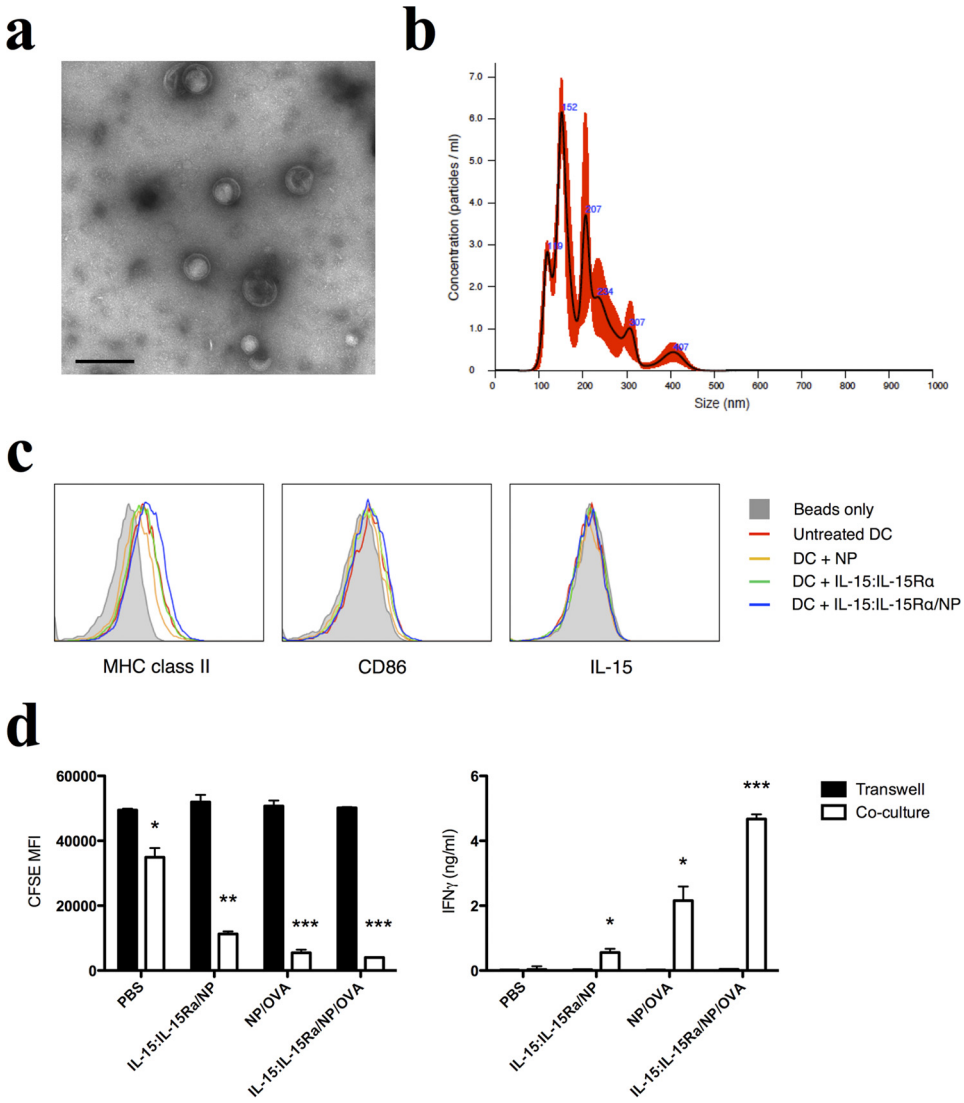

FIGURE 7. **IL-15 is not associated with DC-derived exosomes.** *a*, exosome preparations were visualized by TEM. *Scale bar* = 200 nm. A representative image is shown. *b*, representative size distribution plot of exosomes sized using nanoparticle tracking analysis. *Black line*, mean; *red*, error bars. *c*, exosome-associated proteins were analyzed by flow cytometry. Exosomes were adsorbed to aldehyde/sulfate beads and stained for MHC class II, CD86, and IL-15. *d*, NP-loaded DCs were assayed for their ability to stimulate antigen-specific T cell activation via exosomes. DCs were used to stimulate CFSE-labeled T cells either separated by a transwell (*Transwell*, *black columns*) or in direct cell contact (*Co-culture*, *white columns*). T cells were assayed for CFSE dilution (*left panel*) and IFN-γ secretion. The differences in mean values between the co-culture and Transwell experiments for each condition were compared using an unpaired *t*-test. *** indicates a significance level of $p \leq 0.001$, ** indicates $p \leq 0.01$, and * indicates $p \leq 0.05$.

T cell expansion, survival, and function. Our data indicated that IL-15:IL-15Rα-bearing, antigen-loaded NPs are able to enhance specific T cell responses, transferring IL-15:IL-15Rα molecules to the DC surface in a manner dependent on the NP surface density of IL-15:IL-15Rα but independent of NP internalization, antigen processing, and DC signaling. This effect echoes the physiological mechanism of action of IL-15, which is trans-presented on the surface of activated monocytes and DCs via binding to membrane-bound IL-15Rα (13). Therefore, we wanted to understand what happens when IL-15 is presented in a physiological fashion in a fully functioning system with specified parameters. To do so, we designed a nanoparticle-based antigen-presenting cell that provides all of the essential signals for T cell stimulation: MHC-complexed SIINFEKL for antigen presentation, anti-CD28 antibodies for costimulation, and the presence or absence of trans-presented IL-15:IL-15Rα as the cytokine signal (Fig. 9*a*). We have demonstrated previously that an aAPC system consisting of antigen presentation, costimulation, and cytokine secretion is able to efficiently expand target T cell populations (16, 91).

To assess the difference in levels of T cell stimulation by natural *versus* artificial APCs, we compared the ability of both systems to stimulate 1×10^5 OT-I $CD8^+$ T cells under conditions of equivalent antigen presentation. To equalize antigen presentation between NP-loaded DCs and aAPCs, we loaded DCs with 0.1 mg/ml NP/OVA. Because DCs produce one SIINFEKL-presenting MHC for every ~3000 OVA proteins processed (92), this level of NP/OVA loading produces peptide:MHC on the order of 1 nM. We therefore compared the following T cell stimulation systems: DCs that internalized hetIL-15-coated, antigen-loaded NPs and aAPCs coated with hetIL-15 and 1 nM each of SIINFEKL:MHC and anti-CD28 (Fig. 9*b*). The

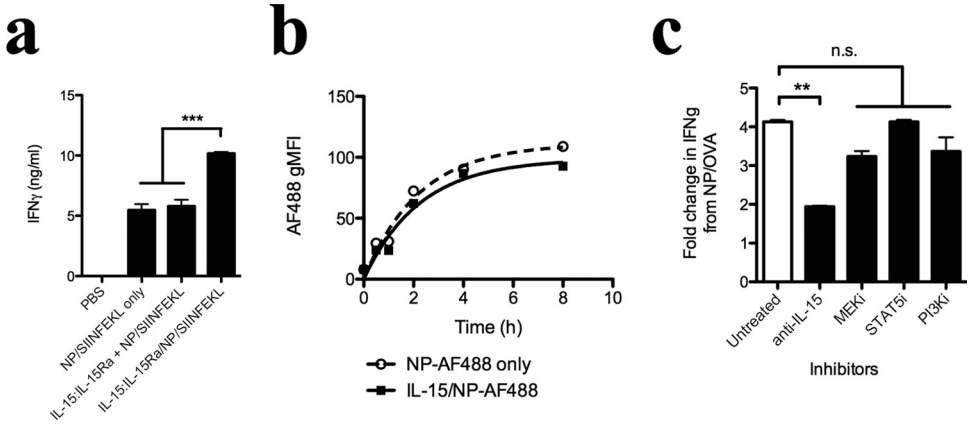

FIGURE 8. **The enhancement of CD8$^+$ T cell activation by coordinated delivery of IL-15:IL-15Rα is independent of antigen processing, nanoparticle internalization, or signaling pathways downstream of the IL-2/15Rβγ receptor.** *a*, To test the requirement for antigen processing, nanoparticles encapsulating the ovalbumin-derived SIINFEKL peptide were loaded into murine bone marrow-derived dendritic cells and used to stimulate OT-I CD8 T cells. *b*, to test the effect of IL-15 on nanoparticle uptake, Alexa Fluor 488-labeled nanoparticles were incubated with DCs in the presence or absence of surface-bound IL-15:IL-15Rα. DCs were fixed and analyzed by flow cytometry at various time points after addition of particles. *c*, DCs were incubated with signaling pathway inhibitors for 2 h prior to nanoparticle uptake, washed, and incubated overnight with OVA-encapsulating nanoparticles in the presence or absence of surface-presented IL-15:IL-15Rα. DCs were then washed and co-incubated with OT-I CD8$^+$ T cells. Data are presented as the resulting -fold increase in IFN-γ when IL-15:IL-15Rα is added to the surface of OVA-encapsulating nanoparticles. Data were analyzed by a one-way ANOVA and a Tukey post-hoc test. *** indicates a significance level of $p \leq 0.001$, ** indicates a significance level of $p \leq 0.01$, and *n.s.* indicates that differences are not statistically significant.

same mass of NP and amount of IL-15 were used for each system.

Both systems stimulated CD8$^+$ T cell proliferation and led to IFN-γ secretion. However, aAPCs stimulated greater cell proliferation and lower IFN-γ production compared with NP-loaded DCs (Fig. 9*c*). These differences may reflect changes in the molecular composition and physical aspects of the natural and artificial APCs.

We then examined the effect of IL-15 presentation on our aAPC system. Equimolar concentrations of SIINFEKL-loaded MHC dimers and anti-CD28 were titrated onto a fixed concentration of nanoparticles that were then used to stimulate OT-I CD8$^+$ T cells in the presence or absence of a fixed concentration of IL-15:IL-15Rα added to the nanoparticle surface. In the absence of IL-15:IL-15Rα, maximal T cell proliferation of 1×10^4 cells occurred at about 10 nM peptide:MHC. In the presence of IL-15:IL-15Rα, a maximal proliferation of 1.5×10^4 cells occurred at 1 nM peptide:MHC, representing a 10-fold increase in T cell sensitivity to antigen and a 50% increase in the magnitude of response (Fig. 9*d*, *left panel*). Similarly, the antigen concentration required for maximal IFN-γ secretion was reduced from 30 to 10 nM peptide:MHC with the addition of IL-15:IL-15Rα, although the highest amount of IFN-γ produced remained the same (Fig. 9*d*, *right panel*). This demonstrated the ability of trans-presented IL-15:IL-15Rα to improve the sensitivity and magnitude of the antigen-specific CD8$^+$ T cell response.

Besides IL-15, another critical cytokine provided by APCs to T cells is IL-2. IL-2 and IL-15 share two of three receptor chains and identical signaling pathways but effect different responses in immunity through differential receptor distribution and modes of action (79, 93–95). IL-15 is trans-presented on the surface of activated monocytes and DCs, whereas IL-2 is secreted in a paracrine fashion from DCs or helper T cells. We hypothesized that the physiological presentation of both IL-15 and IL-2, through the trans-presentation of IL-15 and paracrine delivery of IL-2, can combine the effects of both cytokines to improve the T cell response in our aAPC system. We tested this by adding two different components to our system: exogenous IL-2 at a concentration of 0.5 ng/ml and encapsulating IL-2 within our PLGA nanoparticles at a concentration of 5 ng/mg PLGA. Without IL-15, exogenous IL-2 improves the CD8 response to approximately the same level as when IL-15:IL-15Rα was added, with a maximum proliferation of 1.5×10^4 cells at 1 nM peptide:MHC. Addition of IL-15:IL-15Rα on the surface of the aAPCs further improves this to 2.1×10^4 cells at 0.45 nM (Fig. 9*e*, *left panel*). A slight increase in the sensitivity of IFN-γ production (from 3.6 to 3.1 nM peptide:MHC) was also observed (Fig. 9*e*, *right panel*). Encapsulated IL-2 is a powerful stimulant for T cell proliferation (16, 96). Without IL-15:IL-15Rα, responding T cells peaked at 0.7 nM peptide:MHC for 2.6×10^4 cells, whereas the addition of IL-15:IL-15Rα increased the response still further to 2.9×10^4 cells at 0.35 nM peptide:MHC, effectively doubling the sensitivity of T cells to antigen compared with encapsulated IL-2 alone (Fig. 9*f*, *left panel*). The addition of encapsulated IL-2 appeared to saturate the IFN-γ response, resulting in greatly increased maximal cytokine production but no change in antigen sensitivity of IFN-γ production (Fig. 9*f*, *right panel*). Our results demonstrate that IL-15:IL-15Rα is able to synergize with paracrine delivered IL-2 to enhance T cell activation.

IL-15:IL-15Rα and Encapsulated Antigen Synergize to Delay Tumor Kinetics in an in Vivo Melanoma Model—We evaluated the *in vivo* effects of varying IL-15 trans-presentation during nanoparticle-mediated antigen delivery by testing various NP configurations in the treatment of an aggressive murine melanoma model. We first tested whether IL-15:IL-15Rα synergizes with antigen delivery to stimulate anti-tumor responses *in vivo*. C57Bl/6 mice were challenged intravenously with 1×10^5 B16 melanoma cells expressing ovalbumin (B16-OVA) and then treated systemically with three different IL-15:IL-15Rα configurations: free IL-15:IL-15Rα, IL-15:IL-15Rα/NP, and IL-15:IL-

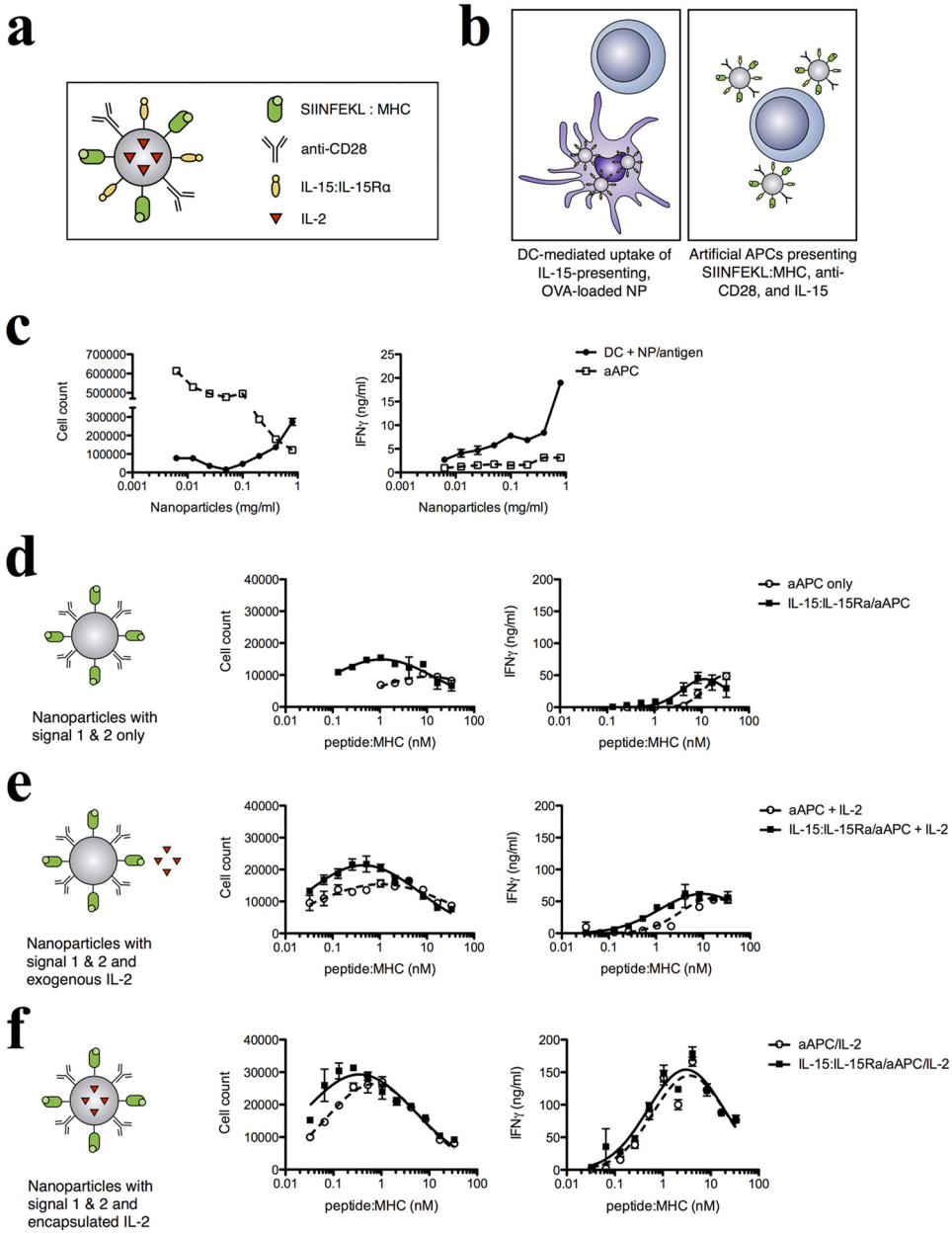

FIGURE 9. **Trans-presented IL-15 improves the sensitivity and magnitude of the antigen-specific CD8$^+$ response and synergizes with additional cytokine signals.** *a*, a nanoparticle-based artificial APC was used to investigate the effect of surface-retained IL-15:IL-15Rα on antigen presentation. *b*, aAPCs were compared with DCs loaded with antigen-encapsulating NPs for their ability to stimulate CD8$^+$ T cells. *c*, T cell stimulation was assessed by cell proliferation (*left panel*) and IFN-γ secretion (*right panel*). Next we assessed the effect of IL-15 trans-presentation on aAPCs. Biotinylated, SIINFEKL-loaded H2-Kb MHC I dimers were titrated on all nanoparticle groups along with equimolar concentrations of anti-CD28. This was done in the presence or absence of surface-bound IL-15:IL-15Rα. The resulting constructs were co-incubated with OT-I CD8$^+$ T cells, and T cell proliferation was assessed. *d*—*f*, data for cell proliferation (*left panels*) and IFN-γ secretion (*right panels*) are shown for three different experiments: blank nanoparticles (*d*), blank nanoparticles with 5 ng/ml of exogenous IL-2 (*e*), and nanoparticles encapsulating 0.5 ng/mg of encapsulated IL-2 (*f*).

15Rα/NP/OVA. Only the third configuration co-delivered IL-15 together with antigen. Control groups were given either PBS or blank nanoparticles alone. Although survival was not improved significantly between free and NP-bound IL-15:IL-15Rα, the addition of encapsulated OVA led to a significant increase in survival (Fig. 10*a*). IL-15:IL-15Rα can therefore synergize with antigen delivery in the anti-tumor immune response.

We next tested the specific configuration of IL-15 and OVA necessary for anti-tumor responses. C57Bl/6 mice were inoculated subcutaneously with 0.5×10^6 B16-OVA cells and then treated systemically with IL-15:IL-15Rα and ovalbumin antigen in four different configurations: soluble IL-15:IL-15Rα and OVA protein only; trans-presented IL-15:IL-15Rα and soluble OVA (IL-15:IL-15Rα/NP + OVA); soluble IL-15:IL-15Rα and encapsulated OVA (IL-15:IL-15Rα + NP/OVA); and trans-presented IL-15:IL-15Rα on NPs encapsulating OVA (IL-15:IL-15Rα/NP/OVA). A control group was treated with blank nanoparticles only. The IL-15:IL-15Rα/NP/OVA particles significantly extended the survival of treated mice compared with other configurations of IL-15:IL-15Rα and ovalbumin (Fig. 10*b*). Notably, configurations where either IL-15:IL-15Rα or OVA was detached from the NPs did not enhance animal sur-

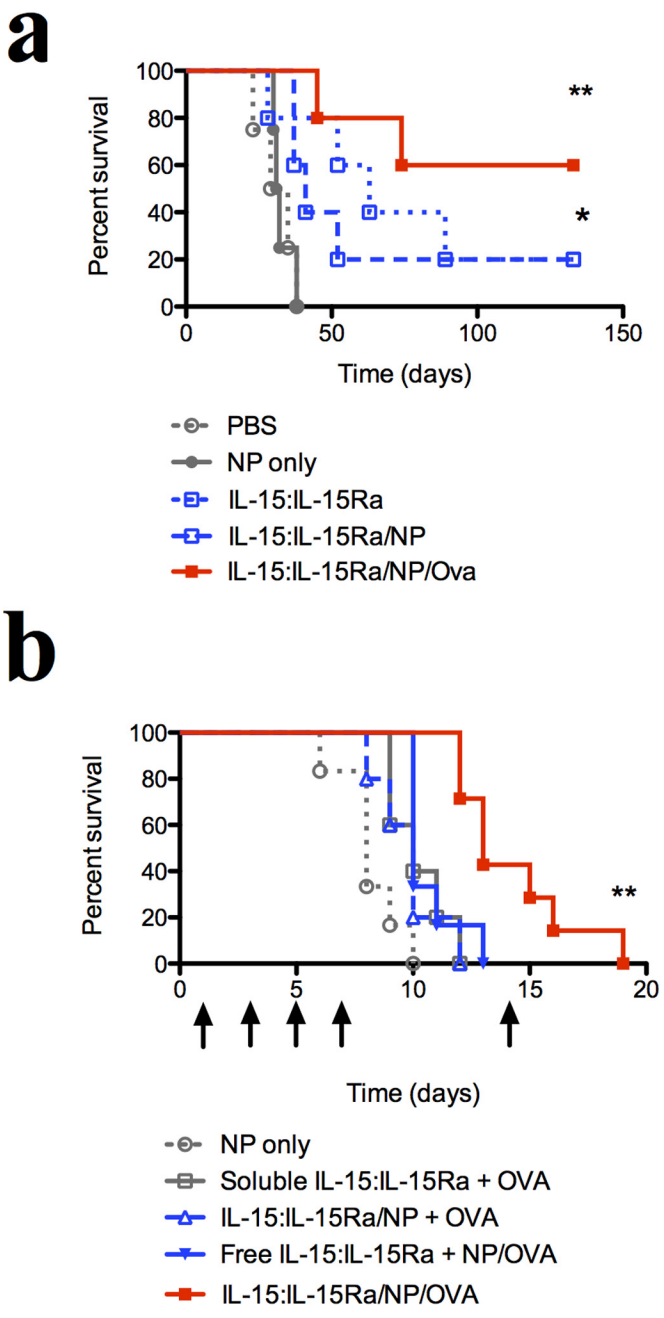

FIGURE 10. ***In vivo* effect of trans-presented IL-15 and encapsulated antigen in a melanoma model.** To test the adjuvant effects of surface-presented IL-15:IL-15Rα *in vivo*, we used a B16 melanoma model. *a*, C57Bl/6 mice were injected intravenously with 1×10^5 OVA-expressing B16 melanoma cells (B16-OVA) to establish pulmonary tumor nodules ($n = 5$ mice/group). 1 day, 2 days, and 10 days after B16-OVA inoculation, mice were injected intraperitoneally with different IL-15:IL-15Rα constructs. Mice were sacrificed upon signs of pulmonary distress. Survival curves were compared against the negative control (PBS) using the Mantel-Cox test. ** indicates a significance level of $p \leq 0.01$, and * indicates $p \leq 0.05$. *b*, to test the effect of IL-15 configuration, mice were inoculated subcutaneously with 0.5×10^6 OVA-expressing B16 melanoma cells. Doses of nanoparticle or IL-15 constructs were injected intraperitoneally on days 1, 3, 5, 7, and 14 after tumors reached a minimum diameter of 4 mm. *Arrows* indicate treatment times ($n = 6$ mice/group). Tumors were measured every other day, and mice were sacrificed when tumors exceeded 15 mm in greatest diameter. Survival curves were compared by Mantel-Cox and Gehan-Breslow-Wilcoxon analysis. Survival curves were compared against the negative control (NP only) using the Mantel-Cox test. ** indicates a significance level of $p \leq 0.01$ for the IL-15:IL-15Ra/NP/OVA group.

vival beyond the control group. Our findings align with recent literature showing that OVA vaccination requires an adjuvant to potentiate antigen-specific protective immunity (97–100) and further highlight the importance of adjuvant configuration in the case of IL-15. Overall, we show that nanoparticles trans-presenting IL-15:IL-15Rα and encapsulating antigen demonstrate *in vivo* efficacy in the treatment of an aggressive model of murine melanoma.

Discussion

We highlight in this work the effect of the mode of cytokine delivery on the immune response specifically with respect to IL-15 signaling. IL-15:IL-15Rα on nanoparticle scaffolds enhances the sensitivity and magnitude of the antigen-specific stimulation of $CD8^+$ T cells upon stimulation by nanoparticle-treated DCs. Our experiments highlight, we believe for the first time, the configuration-dependent delivery of IL-15:IL-15Rα as a key factor for its biological action: that its presentation on the surface of a nanoparticle or cell leads to enhancement of its adjuvant effect. Several groups have previously compared the effects of soluble and trans-presented IL-15, but most compared the action of IL-15 in the presence or absence of cells or scaffolds presenting IL-15Rα (17, 48, 101). However, because IL-15Rα enhances activity when bound to IL-15 (11, 44, 55, 56), these studies could not differentiate between the topological effects of IL-15 from the agonist behavior of IL-15Rα. Mortier *et al.* (47) have compared the activation of natural killer cells by DC supernatants containing IL-15:IL-15Rα and DCs trans-presenting the same, although the membrane-bound concentration of IL-15:IL-15Rα was unknown. Giron-Michel *et al.* (102) have demonstrated differential signaling and functions between soluble and membrane-bound IL-15:IL-15Rα in human hematopoietic progenitor cells, although IL-15 was not controlled for concentration and the membrane-bound form of IL-15 investigated was a novel form complexed with the βγ receptors. By showing that the same quantity of IL-15:IL-15Rα delivered to DCs can differentially affect responding T cells, we show that the action of IL-15:IL-15Rα can be regulated by its configuration during delivery or presentation to cells. Because IL-15:IL-15Rα is physiologically present in both membrane-bound and soluble forms, our work suggests the increased efficacy of surface-presented IL-15:IL-15Rα as an explanation for why the major effects of IL-15 are dependent on its trans-presentation on cell membranes.

We observed that the retention of functional IL-15:IL-15Rα on the surface of DCs is a mechanism for the nano-adjuvant behavior seen with our IL-15:IL-15Rα constructs. The nanoparticle-bound IL-15:IL-15Rα is transferred to the DC cell surface, where it stimulates $CD8^+$ T cells alongside peptide:MHC engagement (Fig. 11*a*). IL-15Rα and IL-2Rα have been observed previously to co-localize with class I and class II MHC in supramolecular receptor clusters, supporting our observation that the transfer of IL-15:IL-15Rα to the DC membrane could enhance the sensitivity and magnitude of T cell stimulation (103). Three mechanisms could account for this IL-15-mediated adjuvant behavior: the scaffolding of IL-15:IL-15Rα to the DC membrane by nanoparticles, the recycling of IL-15:IL-15Rα to the DC membrane after nanoparticle internaliza-

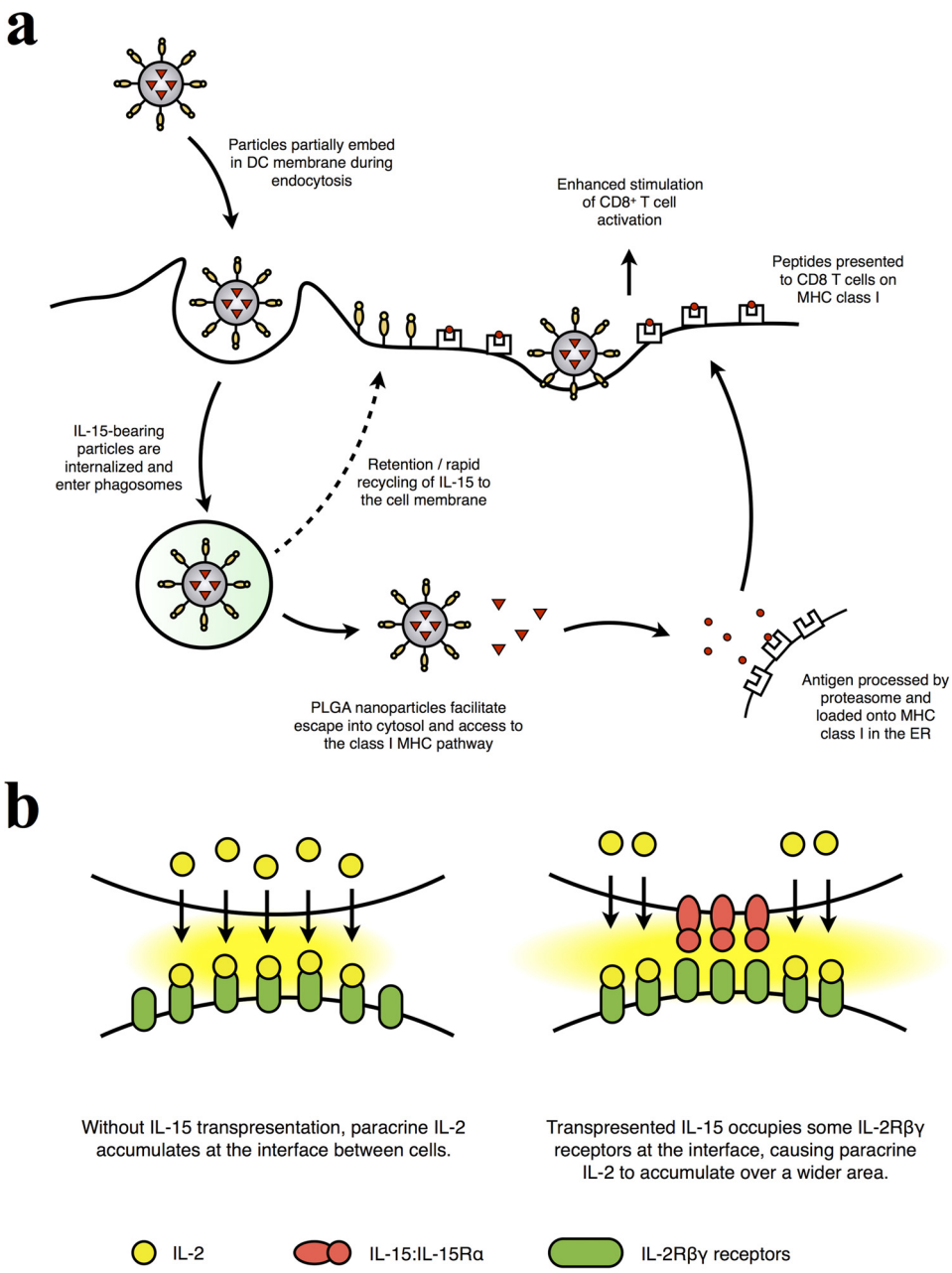

FIGURE 11. **Proposed mechanism of adjuvant IL-15:IL-15Rα action.** *a*, the IL-15:IL-15Rα on nanoparticles synergizes with encapsulated antigen to stimulate antigen-specific $CD8^+$ T cells. As nanoparticles are internalized, they embed in the cell membrane, presenting IL-15:IL-15Rα on the cell surface. Alternatively, IL-15:IL-15Rα could also be recycled to the DC membrane after it enters the nedosome. The PLGA nanoparticles aid in endosomal escape and cross-presentation of antigen on MHC class I. At the DC surface, IL-15:IL-15Rα directly stimulates $CD8^+$ T cells and enhances their sensitivity to DC-presented antigen. *b*, IL-15:IL-15Rα trans-presentation at the cell-NP interface may enhance interfacial IL-2 accumulation. The close apposition of an interacting cell and IL-2-releasing nanoparticle normally leads to accumulation of IL-2 at the cell-NP interface. However, the addition of trans-presented IL-15:IL-15Rα engages a portion of the IL-2Rβγ receptors at the interface, reducing the number of receptors available for IL-2 binding and forcing IL-2 to accumulate over a wider area. This effectively increases the total number of activated IL-2Rβγ receptors in the cell-NP interaction because the signaling induced by IL-15:IL-15Rα trans-presentation and IL-2 binding is identical.

tion, or export of IL-15 to T cells via DC-derived exosomes. The mechanism of NP-mediated scaffolding is supported by the observations that NPs accumulate at the cell membrane (104, 105). Indeed, avidin binding sites could be detected on the DC surface shortly after addition of untreated NPs (Fig. 6*d*), and the nonspecific interaction of NPs with the DC membrane is supported by our observation that fixed DCs can present bioactive IL-15 (Fig. 6, *e* and *f*). Alternatively, studies by Waldmann and co-workers (13, 48) have suggested that IL-15 and IL-15Rα are recycled and stored intracellularly after internalization, indicating that IL-15 may be transported to the cell membrane after NP uptake, which may explain the longevity of surface-retained IL-15 on DCs in our experiments. We showed that intraendosomally delivered IL-15 could be detected after internalization, where it may survive to be recycled to the cell membrane. Finally, previous work has shown that IL-15Rα associated with DC-derived exosomes can stimulate natural killer cells, leading to proliferation and IFN-γ production (88). However, in our

system, we did not observe proliferation or IFN-γ being produced from $CD8^+$ transwell cultures, nor did we observe exosome-associated IL-15 (Fig. 7).

In our use of the artificial APC system to elucidate the mechanism of action of our NP-loaded DCs, we noted that the two systems generated differential responses. Although we observed increased proliferation with aAPCs compared with NP-loaded DCs, that trend is reversed when we examined IFN-γ levels. Antigen-specific proliferation and IFN-γ release can be dissociated from each other in clonotypic activation of T cells in murine lines and in immune responses from splenic T cells (106, 107). In addition, the presence of low levels of IL-2 can enhance IFN-γ secretion independent of proliferation (107). We detected the presence of IL-2 produced in the case of NP-loaded DCs but not from aAPCs (data not shown), which may contribute to the higher levels of IFN-γ seen with NP-loaded DCs. aAPCs provide a very strong stimulus for T cell proliferation (16, 96, 108) and, indeed, outperform NP-loaded DCs in expanding T cells. We note that artificial APCs are by no means equivalent to natural DCs in terms of the breadth and intensity of immune responses triggered. However, by providing a basic approximation of antigen recognition, co-stimulation, and cytokine signaling, the utility of aAPCs for elucidating immune mechanisms is demonstrated in this work.

Our work affirms that the physiological presentation of IL-15 and IL-2 is important for their action on T cells. Use of the IL-15:IL-15Rα complex and paracrine delivery of IL-2 were shown to better activate T cells than if either cytokine were delivered alone and could stimulate even stronger responses if delivered in combination in our aAPC system. We have previously described this phenomenon for IL-2 (16, 96) and modeled the interaction of paracrine IL-2 with a receiving cell under a variety of conditions (71, 109–110), which provides a basis for understanding how these two cytokines would interact with one another. When an aAPC releases a cytokine such as IL-2, mathematical modeling indicates that IL-2 accumulates significantly at the particle:cell interface. Locally concentrated IL-2 would bind readily to available IL-2/15βγ receptors, thereby enhancing T cell activation. If trans-presented IL-15:IL-15Rα were present at the particle:cell interface, it would occupy a portion of the IL-2/15βγ receptors, allowing the local concentration of IL-2 to increase further. Such receptor occupancy would not hinder cytokine-induced T cell activation because the signaling ends of IL-2/15βγ are the same whether bound to IL-2 or IL-15:IL-15Rα (93); nor would the number of IL-2/15βγ receptors decrease because engagement by trans-presented IL-15:IL-15Rα does not trigger significant down-regulation of IL-2/15βγ (42). The combined action of physiologically presented IL-2 and IL-15 would therefore continue to increase T cell activation until available IL-2/15βγ receptors are saturated (Fig. 11*b*). These results shed more light on the interaction between IL-2 and IL-15 and show that the cytokines can be combined to stimulate robust T cell responses at levels below receptor saturation. These findings could have implications for the design of IL-2- and IL-15-based immunotherapies.

Multiple clinical trials for single-chain IL-15 and heterodimeric IL-15 are currently recruiting or underway. Initial results from the first-in-human phase I trial of single-chain IL-15 indicate a modest form of capillary leak that was less severe than that induced by IL-2 but also moderate toxicities, including hypotension and thrombocytopenia (52). In light of the significant clinical interest behind IL-15, our findings provide new strategies for optimizing its therapeutic delivery, aimed at maximizing its effectiveness while limiting its associated toxicities. Our results have particular significance in the application of IL-15 to therapeutic cancer vaccines where the nanoparticle-mediated combination delivery of IL-15 and antigen to target DCs may prove to be a useful strategy.

Author Contributions—E. H., T. M. F., and R. A. F. conceived the study. E. H. and T. M. F. designed the experiments, coordinated the study, and wrote the paper. E. H. performed the experiments and analyzed the data for Figs. 1 and 6–9. E. H. and I. M. U. performed the experiments and analyzed the data for Figs. 2–4 and 10. D. J. H. performed the experiment shown in Fig. 5. C. B. and G. N. P. provided the heterodimeric IL-15 used in all experiments. S. J. provided the SIINFEKL:MHC used in the artificial APC experiments. All authors critically reviewed and approved the final version of the manuscript.

Acknowledgments—We thank Drs. Lieping Chen and Frederick Sigworth for critical reading of the manuscript and many helpful discussions. We also thank Drs. Donoven Kim and Michael McHugh for assistance with the animal experiments, Ewa Menet and Geoffrey Lyon (Yale Immunobiology Flow Cytometry Core), and Dr. Xinran Liu (Yale School of Medicine Electron Microscopy Core) for technical assistance.

References

1. Banchereau, J., and Steinman, R. M. (1998) Dendritic cells and the control of immunity. *Nature* **392,** 245–252
2. Steinman, R. M., and Banchereau, J. (2007) Taking dendritic cells into medicine. *Nature* **449,** 419–426
3. Théry, C., and Amigorena, S. (2001) The cell biology of antigen presentation in dendritic cells. *Curr. Opin. Immunol.* **13,** 45–51
4. Mahnke, K., Guo, M., Lee, S., Sepulveda, H., Swain, S. L., Nussenzweig, M., and Steinman, R. M. (2000) The dendritic cell receptor for endocytosis, DEC-205, can recycle and enhance antigen presentation via major histocompatibility complex class II-positive lysosomal compartments. *J. Cell Biol.* **151,** 673–684
5. Sallusto, F., Cella, M., Danieli, C., and Lanzavecchia, A. (1995) Dendritic cells use macropinocytosis and the mannose receptor to concentrate macromolecules in the major histocompatibility complex class II compartment: downregulation by cytokines and bacterial products. *J. Exp. Med.* **182,** 389–400
6. Savina, A., and Amigorena, S. (2007) Phagocytosis and antigen presentation in dendritic cells. *Immunol. Rev.* **219,** 143–156
7. Engering, A. J., Cella, M., Fluitsma, D., Brockhaus, M., Hoefsmit, E. C., Lanzavecchia, A., and Pieters, J. (1997) The mannose receptor functions as a high capacity and broad specificity antigen receptor in human dendritic cells. *Eur. J. Immunol.* **27,** 2417–2425
8. Banchereau, J., Briere, F., Caux, C., Davoust, J., Lebecque, S., Liu, Y.-J., Pulendran, B., and Palucka, K. (2000) Immunobiology of dendritic cells. *Annu. Rev. Immunol.* **18,** 767–811
9. Malek, T. R. (2008) The Biology of Interleukin-2. *Annu. Rev. Immunol.* **26,** 453–479
10. Huse, M., Lillemeier, B. F., Kuhns, M. S., Chen, D. S., and Davis, M. M. (2006) T cells use two directionally distinct pathways for cytokine secretion. *Nat. Immunol.* **7,** 247–255
11. Bergamaschi, C., Rosati, M., Jalah, R., Valentin, A., Kulkarni, V., Alicea, C., Zhang, G. M., Patel, V., Felber, B. K., and Pavlakis, G. N. (2008) Intracellular interaction of interleukin-15 with its receptor α during produc-

tion leads to mutual stabilization and increased bioactivity. *J. Biol. Chem.* **283,** 4189–4199
12. Stonier, S. W., and Schluns, K. S. (2010) Trans-presentation: A novel mechanism regulating IL-15 delivery and responses. *Immunol. Lett.* **127,** 85–92
13. Dubois, S., Mariner, J., Waldmann, T. A., and Tagaya, Y. (2002) IL-15Ra recycles and presents IL-15 in *trans* to neighboring cells. *Immunity* **17,** 537–547
14. Bergamaschi, C., Bear, J., Rosati, M., Beach, R. K., Alicea, C., Sowder, R., Chertova, E., Rosenberg, S. A., Felber, B. K., and Pavlakis, G. N. (2012) Circulating IL-15 exists as heterodimeric complex with soluble IL-15Rα in human and mouse serum. *Blood* **120,** e1–8
15. Chertova, E., Bergamaschi, C., Chertov, O., Sowder, R., Bear, J., Roser, J. D., Beach, R. K., Lifson, J. D., Felber, B. K., and Pavlakis, G. N. (2013) Characterization and favorable *in vivo* properties of heterodimeric soluble IL-15: IL-15Rα cytokine compared with IL-15 monomer. *J. Biol. Chem.* **288,** 18093–18103
16. Steenblock, E. R., Fadel, T., Labowsky, M., Pober, J. S., and Fahmy, T. M. (2011) An artificial antigen-presenting cell with paracrine delivery of IL-2 impacts the magnitude and direction of the T cell response. *J. Biol. Chem.* **286,** 34883–34892
17. Kokaji, A. I., Hockley, D. L., and Kane, K. P. (2008) IL-15 Transpresentation augments CD8+ T cell activation and is required for optimal recall responses by central memory CD8+ T cells. *J. Immunol.* **180,** 4391–4401
18. Elamanchili, P., Diwan, M., Cao, M., and Samuel, J. (2004) Characterization of poly(*d,l*-lactic-co-glycolic acid) based nanoparticulate system for enhanced delivery of antigens to dendritic cells. *Vaccine* **22,** 2406–2412
19. Cho, N.-H., Cheong, T.-C., Min, J. H., Wu, J. H., Lee, S. J., Kim, D., Yang, J.-S., Kim, S., Kim, Y. K., and Seong, S.-Y. (2011) A multifunctional core-shell nanoparticle for dendritic cell-based cancer immunotherapy. *Nature Nantechnol.* **6,** 675–682
20. Villa, C. H., Dao, T., Ahearn, I., Fehrenbacher, N., Casey, E., Rey, D. A., Korontsvit, T., Zakhaleva, V., Batt, C. A., Philips, M. R., and Scheinberg, D. A. (2011) Single-walled carbon nanotubes deliver peptide antigen into dendritic cells and enhance IgG responses to tumor-associated antigens. *ACS Nano* **5,** 5300–5311
21. De Koker, S., De Geest, B. G., Singh, S. K., De Rycke, R., Naessens, T., van Kooyk, Y., Demeester, J., De Smedt, S. C., and Grooten, J. (2009) Polyelectrolyte microcapsules as antigen delivery vehicles to dendritic cells: uptake, processing, and cross-presentation of encapsulated antigens. *Angew. Chem. Int. Ed. Engl.* **48,** 8485–8489
22. Hamdy, S., Haddadi, A., Hung, R. W., and Lavasanifar, A. (2011) Targeting dendritic cells with nano-particulate PLGA cancer vaccine formulations. *Adv. Drug Delivery Rev.* **63,** 943–955
23. Klippstein, R., and Pozo, D. (2010) Nanotechnology-based manipulation of dendritic cells for enhanced immunotherapy strategies. *Nanomedicine* **6,** 523–529
24. Akagi, T., Baba, M., and Akashi, M. (2012) in *Polymers in Nanomedicine* (Kunugi, S., and Yamaoka, T. eds.) pp 31–64, Springer, Berlin
25. Hrkach, J., Von Hoff, D., Mukkaram Ali, M., Andrianova, E., Auer, J., Campbell, T., De Witt, D., Figa, M., Figueiredo, M., Horhota, A., Low, S., McDonnell, K., Peeke, E., Retnarajan, B., Sabnis, A., Schnipper, E., Song, J. J., Song, Y. H., Summa, J., Tompsett, D., Troiano, G., Van Geen Hoven, T., Wright, J., LoRusso, P., Kantoff, P. W., Bander, N. H., Sweeney, C., Farokhzad, O. C., Langer, R., and Zale, S. (2012) Preclinical development and clinical translation of a PSMA-targeted docetaxel nanoparticle with a differentiated pharmacological profile. *Sci. Transl. Med.* **4,** 128ra39
26. Park, J., Fong, P. M., Lu, J., Russell, K. S., Booth, C. J., Saltzman, W. M., and Fahmy, T. M. (2009) PEGylated PLGA nanoparticles for the improved delivery of doxorubicin. *Nanomedicine* **5,** 410–418
27. Cheng, J., Teply, B. A., Sherifi, I., Sung, J., Luther, G., Gu, F. X., Levy-Nissenbaum, E., Radovic-Moreno, A. F., Langer, R., and Farokhzad, O. C. (2007) Formulation of functionalized PLGA-PEG nanoparticles for *in vivo* targeted drug delivery. *Biomaterials* **28,** 869–876
28. Sadat Tabatabaei Mirakabad, F., Nejati-Koshki, K., Akbarzadeh, A., Yamchi, M. R., Milani, M., Zarghami, N., Zeighamian, V., Rahimzadeh, A., Alimohammadi, S., Hanifehpour, Y., and Joo, S. W. (2014) PLGA-based nanoparticles as cancer drug delivery systems. *Asian Pacific Journal of Cancer Prevention* **15,** 517–535
29. Danhier, F., Ansorena, E., Silva, J. M., Coco, R., Le Breton, A., and Préat, V. (2012) PLGA-based nanoparticles: an overview of biomedical applications. *J. Control. Release* **161,** 505–522
30. Lü, J.-M., Wang, X., Marin-Muller, C., Wang, H., Lin, P. H., Yao, Q., and Chen, C. (2009) Current advances in research and clinical applications of PLGA-based nanotechnology. *Expert Rev. Mol. Diagn.* **9,** 325–341
31. Walter, E., Dreher, D., Kok, M., Thiele, L., Kiama, S. G., Gehr, P., and Merkle, H. P. (2001) Hydrophilic poly(DL-lactide-co-glycolide) microspheres for the delivery of DNA to human-derived macrophages and dendritic cells. *J. Control. Release* **76,** 149–168
32. Bandyopadhyay, A., Fine, R. L., Demento, S., Bockenstedt, L. K., and Fahmy, T. M. (2011) The impact of nanoparticle ligand density on dendritic-cell targeted vaccines. *Biomaterials* **32,** 3094–3105
33. Demento, S. L., Bonafé, N., Cui, W., Kaech, S. M., Caplan, M. J., Fikrig, E., Ledizet, M., and Fahmy, T. M. (2010) TLR9-targeted biodegradable nanoparticles as immunization vectors protect against West Nile encephalitis. *J. Immunol.* **185,** 2989–2997
34. Demento, S. L., Eisenbarth, S. C., Foellmer, H. G., Platt, C., Caplan, M. J., Saltzman, W. M., Mellman, I., Ledizet, M., Fikrig, E., Flavell, R. A., and Fahmy, T. M. (2009) Inflammasome-activating nanoparticles as modular systems for optimizing vaccine efficacy. *Vaccine* **27,** 3013–3021
35. Zhang, Z., Tongchusak, S., Mizukami, Y., Kang, Y. J., Ioji, T., Touma, M., Reinhold, B., Keskin, D. B., Reinherz, E. L., and Sasada, T. (2011) Induction of anti-tumor cytotoxic T cell responses through PLGA-nanoparticle mediated antigen delivery. *Biomaterials* **32,** 3666–3678
36. Hamdy, S., Molavi, O., Ma, Z., Haddadi, A., Alshamsan, A., Gobti, Z., Elhasi, S., Samuel, J., and Lavasanifar, A. (2008) Co-delivery of cancer-associated antigen and Toll-like receptor 4 ligand in PLGA nanoparticles induces potent CD8+ T cell-mediated anti-tumor immunity. *Vaccine* **26,** 5046–5057
37. Saluja, S. S., Hanlon, D. J., Sharp, F. A., Hong, E., Khalil, D., Robinson, E., Tigelaar, R., Fahmy, T. M., and Edelson, R. L. (2014) Targeting human dendritic cells via DEC-205 using PLGA nanoparticles leads to enhanced cross-presentation of a melanoma-associated antigen. *Int. J. Nanomedicine* **9,** 5231–5246
38. Solbrig, C. M., Saucier-Sawyer, J. K., Cody, V., Saltzman, W. M., and Hanlon, D. J. (2007) Polymer nanoparticles for immunotherapy from encapsulated tumor-associated antigens and whole tumor cells. *Mol. Pharm.* **4,** 47–57
39. Shen, H., Ackerman, A. L., Cody, V., Giodini, A., Hinson, E. R., Cresswell, P., Edelson, R. L., Saltzman, W. M., and Hanlon, D. J. (2006) Enhanced and prolonged cross-presentation following endosomal escape of exogenous antigens encapsulated in biodegradable nanoparticles. *Immunology* **117,** 78–88
40. Steel, J. C., Waldmann, T. A., and Morris, J. C. (2012) Interleukin-15 biology and its therapeutic implications in cancer. *Trends Pharmacol. Sci.* **33,** 35–41
41. Bergamaschi, C., Jalah, R., Kulkarni, V., Rosati, M., Zhang, G. M., Alicea, C., Zolotukhin, A. S., Felber, B. K., and Pavlakis, G. N. (2009) Secretion and biological activity of short signal peptide IL-15 is chaperoned by IL-15 receptor α *in vivo*. *J. Immunol.* **183,** 3064–3072
42. Perdreau, H., Mortier, E., Bouchaud, G., Solé, V., Boublik, Y., Plet, A., and Jacques, Y. (2010) Different dynamics of IL-15R activation following IL-15 cis- or trans-presentation. *Eur. Cytokine Netw.* **21,** 297–307
43. Sandau, M. M., Schluns, K. S., Lefrancois, L., and Jameson, S. C. (2004) Cutting edge: transpresentation of IL-15 by bone marrow-derived cells necessitates expression of IL-15 and IL-15Ra by the same cells. *J. Immunol.* **173,** 6537–6541
44. Rubinstein, M. P., Kovar, M., Purton, J. F., Cho, J.-H., Boyman, O., Surh, C. D., and Sprent, J. (2006) Converting IL-15 to a superagonist by binding to soluble IL-15Ra. *Proc. Nat. Acad. Sci. U.S.A.* **103,** 9166–9171
45. Bergamaschi, C., Bear, J., Rosati, M., Beach, R. K., Alicea, C., Sowder, R., Chertova, E., Rosenberg, S. A., Felber, B. K., and Pavlakis, G. N. (2012) Circulating interleukin-15 (IL-15) exists as heterodimeric complex with soluble IL-15 receptor α (IL-15R) in human serum. *Blood* **120,** e1-e8
46. Huntington, N. D., Legrand, N., Alves, N. L., Jaron, B., Weijer, K., Plet, A.,

Corcuff, E., Mortier, E., Jacques, Y., Spits, H., and Di Santo, J. P. (2009) IL-15 trans-presentation promotes human NK cell development and differentiation *in vivo*. *J. Exp. Med.* **206,** 25–34
47. Mortier, E., Woo, T., Advincula, R., Gozalo, S., and Ma, A. (2008) IL-15R chaperones IL-15 to stable dendritic cell membrane complexes that activate NK cells via trans presentation. *J. Exp. Med.* **205,** 1213–1225
48. Sato, N., Patel, H. J., Waldmann, T. A., and Tagaya, Y. (2007) The IL-15/IL-15Ra on cell surfaces enables sustained IL-15 activity and contributes to the long survival of CD8 memory T cells. *Proc. Natl. Acad. Sci. U.S.A.* **104,** 588–593
49. Rückert, R., Brandt, K., Bulanova, E., Mirghomizadeh, F., Paus, R., and Bulfone-Paus, S. (2003) Dendritic cell-derived IL-15 controls the induction of CD8 T cell immune responses. *Eur. J. Immunol.* **33,** 3493–3503
50. Jakobisiak, M., Golab, J., and Lasek, W. (2011) Interleukin 15 as a promising candidate for tumor immunotherapy. *Cytokine Growth Factor Rev.* **22,** 99–108
51. Cheever, M. A. (2008) Twelve immunotherapy drugs that could cure cancers. *Immunol. Rev.* **222,** 357–368
52. Conlon, K. C., Lugli, E., Welles, H. C., Rosenberg, S. A., Fojo, A. T., Morris, J. C., Fleisher, T. A., Dubois, S. P., Perera, L. P., Stewart, D. M., Goldman, C. K., Bryant, B. R., Decker, J. M., Chen, J., Worthy, T. A., Figg, W. D., Sr., Peer, C. J., Sneller, M. C., Lane, H. C., Yovandich, J. L., Creekmore, S. P., Roederer, M., and Waldmann, T. A. (2015) Redistribution, hyperproliferation, activation of natural killer cells and CD8 T cells, and cytokine production during first-in-human clinical trial of recombinant human interleukin-15 in patients with cancer. *J. Clin. Oncol.* **33,** 74–82
53. Bessard, A., Solé, V., Bouchaud, G., Quéméner, A., and Jacques, Y. (2009) High antitumor activity of RLI, an interleukin-15 (IL-15)-IL-15 receptor α fusion protein, in metastatic melanoma and colorectal cancer. *Mol. Cancer Ther.* **8,** 2736–2745
54. Epardaud, M., Elpek, K. G., Rubinstein, M. P., Yonekura, A. R., Bellemare-Pelletier, A., Bronson, R., Hamerman, J. A., Goldrath, A. W., and Turley, S. J. (2008) Interleukin-15/interleukin-15R complexes promote destruction of established tumors by reviving tumor-resident CD8+ T cells. *Cancer Res.* **68,** 2972–2983
55. Dubois, S., Patel, H. J., Zhang, M., Waldmann, T. A., and Müller, J. R. (2008) Preassociation of IL-15 with IL-15Ra-IgG1-Fc enhances its activity on proliferation of NK and CD8+/CD44 high T cells and its antitumor action. *J. Immunol.* **180,** 2099–2106
56. Stoklasek, T. A., Schluns, K. S., and Lefrançois, L. (2006) Combined IL-15/IL-15Ra immunotherapy maximizes IL-15 activity *in vivo*. *J. Immunol.* **177,** 6072–6080
57. Boyer, J. D., Robinson, T. M., Kutzler, M. A., Vansant, G., Hokey, D. A., Kumar, S., Parkinson, R., Wu, L., Sidhu, M. K., Pavlakis, G. N., Felber, B. K., Brown, C., Silvera, P., Lewis, M. G., Monforte, J., Waldmann, T. A., Eldridge, J., and Weiner, D. B. (2007) Protection against simian/human immunodeficiency virus (SHIV) 89.6P in macaques after coimmunization with SHIV antigen and IL-15 plasmid. *Proc. Natl. Acad. Sci. U.S.A.* **104,** 18648–18653
58. Kutzler, M. A., Robinson, T. M., Chattergoon, M. A., Choo, D. K., Choo, A. Y., Choe, P. Y., Ramanathan, M. P., Parkinson, R., Kudchodkar, S., Tamura, Y., Sidhu, M., Roopchand, V., Kim, J. J., Pavlakis, G. N., Felber, B. K., Waldmann, T. A., Boyer, J. D., and Weiner, D. B. (2005) Coimmunization with an optimized IL-15 plasmid results in enhanced function and longevity of CD8 T cells that are partially independent of CD4 T cell help. *J. Immunol.* **175,** 112–123
59. Xin, K.-Q., Hamajima, K., Sasaki, S., Tsuji, T., Watabe, S., Okada, E., and Okuda, K. (1999) IL-15 expression plasmid enhances cell-mediated immunity induced by an HIV-1 DNA vaccine. *Vaccine* **17,** 858–866
60. Rubinstein, M. P., Kadima, A. N., Salem, M. L., Nguyen, C. L., Gillanders, W. E., and Cole, D. J. (2002) Systemic administration of IL-15 augments the antigen-specific primary CD8+ T cell response following vaccination with peptide-pulsed dendritic cells. *J. Immunol.* **169,** 4928–4935
61. Saikh, K. U., Kissner, T. L., Nystrom, S., Ruthel, G., and Ulrich, R. G. (2008) Interleukin-15 increases vaccine efficacy through a mechanism linked to dendritic cell maturation and enhanced antibody titers. *Clin. Vaccine Immunol.* **15,** 131–137
62. Tourkova, I. L., Yurkovetsky, Z. R., Gambotto, A., Makarenkova, V. P., Perez, L., Balkir, L., Robbins, P. D., Shurin, M. R., and Shurin, G. V. (2002) Increased function and survival of IL-15-transduced human dendritic cells are mediated by up-regulation of IL-15Ra and Bcl-2. *J. Leukocyte Biol.* **72,** 1037–1045
63. Pulendran, B., Dillon, S., Joseph, C., Curiel, T., Banchereau, J., and Mohamadzadeh, M. (2004) Dendritic cells generated in the presence of GM-CSF plus IL-15 prime potent CD8+ Tc1 responses *in vivo*. *Eur. J. Immunol.* **34,** 66–73
64. Saikh, K. U., Khan, A. S., Kissner, T., and Ulrich, R. G. (2001) IL-15-induced conversion of monocytes to mature dendritic cells. *Clin. Exp. Immunol.* **126,** 447–455
65. Dubsky, P., Saito, H., Leogier, M., Dantin, C., Connolly, J. E., Banchereau, J., and Palucka, A. K. (2007) IL-15-induced human DC efficiently prime melanoma-specific naive CD8+ T cells to differentiate into CTL. *Eur. J. Immunol.* **37,** 1678–1690
66. Tourkova, I. L., Shurin, G. V., Chatta, G. S., Perez, L., Finke, J., Whiteside, T. L., Ferrone, S., and Shurin, M. R. (2005) Restoration by IL-15 of MHC class I Antigen-processing machinery in human dendritic cells inhibited by tumor-derived gangliosides. *J. Immunol.* **175,** 3045–3052
67. Kasturi, S. P., Skountzou, I., Albrecht, R. A., Koutsonanos, D., Hua, T., Nakaya, H. I., Ravindran, R., Stewart, S., Alam, M., Kwissa, M., Villinger, F., Murthy, N., Steel, J., Jacob, J., Hogan, R. J., García-Sastre, A., Compans, R., and Pulendran, B. (2011) Programming the magnitude and persistence of antibody responses with innate immunity. *Nature* **470,** 543–547
68. Demento, S. L., Cui, W., Criscione, J. M., Stern, E., Tulipan, J., Kaech, S. M., and Fahmy, T. M. (2012) Role of sustained antigen release from nanoparticle vaccines in shaping the T cell memory phenotype. *Biomaterials* **33,** 4957–4964
69. Fahmy, T. M., Samstein, R. M., Harness, C. C., and Mark Saltzman, W. (2005) Surface modification of biodegradable polyesters with fatty acid conjugates for improved drug targeting. *Biomaterials* **26,** 5727–5736
70. Bergamaschi, C., Kulkarni, V., Rosati, M., Alicea, C., Jalah, R., Chen, S., Bear, J., Sardesai, N. Y., Valentin, A., Felber, B. K., and Pavlakis, G. N. (2015) Intramuscular delivery of heterodimeric IL-15 DNA in macaques produces systemic levels of bioactive cytokine inducing proliferation of NK and T cells. *Gene Ther.* **22,** 76–86
71. Labowsky, M., and Fahmy, T. M. (2012) Diffusive transfer between two intensely interacting cells with limited surface kinetics. *Chem. Eng. Sci.* **74,** 114–123
72. Inaba, K., Swiggard, W. J., Steinman, R. M., Romani, N., and Schuler, G. (2001) Isolation of dendritic cells. *Curr. Protoc. Immunol.* 10.1002/0471142735.im0307s25
73. Ho, W. Y., Nguyen, H. N., Wolfl, M., Kuball, J., and Greenberg, P. D. (2006) *In vitro* methods for generating CD8+ T-cell clones for immunotherapy from the naïve repertoire. *J. Immunol. Methods* **310,** 40–52
74. Obermaier, B., Dauer, M., Herten, J., Schad, K., Endres, S., and Eigler, A. (2003) Development of a new protocol for 2-day generation of mature dendritic cells from human monocytes. *Biol. Proced. Online* **5,** 197–203
75. Dauer, M., Obermaier, B., Herten, J., Haerle, C., Pohl, K., Rothenfusser, S., Schnurr, M., Endres, S., and Eigler, A. (2003) Mature dendritic cells derived from human monocytes within 48 hours: a novel strategy for dendritic cell differentiation from blood precursors. *J. Immunol.* **170,** 4069–4076
76. Kelly, J. M., Sterry, S. J., Cose, S., Turner, S. J., Fecondo, J., Rodda, S., Fink, P. J., and Carbone, F. R. (1993) Identification of conserved T cell receptor CDR3 residues contacting known exposed peptide side chains from a major histocompatibility complex class I-bound determinant. *Eur. J. Immunol.* **23,** 3318–3326
77. Hirosue, S., Kourtis, I. C., van der Vlies, A. J., Hubbell, J. A., and Swartz, M. A. (2010) Antigen delivery to dendritic cells by poly(propylene sulfide) nanoparticles with disulfide conjugated peptides: cross-presentation and T cell activation. *Vaccine* **28,** 7897–7906
78. Fifis, T., Gamvrellis, A., Crimeen-Irwin, B., Pietersz, G. A., Li, J., Mottram, P. L., McKenzie, I. F., and Plebanski, M. (2004) Size-dependent immunogenicity: therapeutic and protective properties of nano-vaccines against tumors. *J. Immunol.* **173,** 3148–3154
79. Waldmann, T. A. (2006) The biology of interleukin-2 and interleukin-15: implications for cancer therapy and vaccine design. *Nat. Rev. Immunol.*

6, 595–601
80. Teague, R. M., Sather, B. D., Sacks, J. A., Huang, M. Z., Dossett, M. L., Morimoto, J., Tan, X., Sutton, S. E., Cooke, M. P., Ohlén, C., and Greenberg, P. D. (2006) Interleukin-15 rescues tolerant CD8+ T cells for use in adoptive immunotherapy of established tumors. *Nat. Med.* **12,** 335–341
81. Mueller, K., Schweier, O., and Pircher, H. (2008) Efficacy of IL-2- versus IL-15-stimulated CD8 T cells in adoptive immunotherapy. *Eur. J. Immunol.* **38,** 2874–2885
82. Kawakami, Y., Eliyahu, S., Sakaguchi, K., Robbins, P. F., Rivoltini, L., Yannelli, J. R., Appella, E., and Rosenberg, S. A. (1994) Identification of the immunodominant peptides of the MART-1 human melanoma antigen recognized by the majority of HLA-A2-restricted tumor infiltrating lymphocytes. *J. Exp. Med.* **180,** 347–352
83. Johnson, L. A., Heemskerk, B., Powell, D. J., Jr., Cohen, C. J., Morgan, R. A., Dudley, M. E., Robbins, P. F., and Rosenberg, S. A. (2006) Gene transfer of tumor-reactive TCR confers both high avidity and tumor reactivity to nonreactive peripheral blood mononuclear cells and tumor-infiltrating lymphocytes. *J. Immunol.* **177,** 6548–6559
84. Zhu, X., Marcus, W. D., Xu, W., Lee, H. I., Han, K., Egan, J. O., Yovandich, J. L., Rhode, P. R., and Wong, H. C. (2009) Novel human interleukin-15 agonists. *J. Immunol.* **183,** 3598–3607
85. Kim, Y. S., Maslinski, W., Zheng, X. X., Stevens, A. C., Li, X. C., Tesch, G. H., Kelley, V. R., and Strom, T. B. (1998) Targeting the IL-15 receptor with an antagonist IL-15 mutant/Fcγ2a protein blocks delayed-type hypersensitivity. *J. Immunol.* **160,** 5742–5748
86. Ding, Z., Fong, R. B., Long, C. J., Stayton, P. S., and Hoffman, A. S. (2001) Size-dependent control of the binding of biotinylated proteins to streptavidin using a polymer shield. *Nature* **411,** 59–62
87. Noppl-Simson, D. A., and Needham, D. (1996) Avidin-biotin interactions at vesicle surfaces: adsorption and binding, cross-bridge formation, and lateral interactions. *Biophys. J.* **70,** 1391–1401
88. Viaud, S., Terme, M., Flament, C., Taieb, J., André, F., Novault, S., Escudier, B., Robert, C., Caillat-Zucman, S., Tursz, T., Zitvogel, L., and Chaput, N. (2009) Dendritic cell-derived exosomes promote natural killer cell activation and proliferation: a role for NKG2D ligands and IL-15Rα. *PLoS ONE* **4,** e4942
89. Théry, C., Amigorena, S., Raposo, G., and Clayton, A. (2006) Isolation and characterization of exosomes from cell culture supernatants and biological fluids. *Curr. Protoc. Cell Biol.* 10.1002/0471143030.cb0322s30
90. Zitvogel, L., Regnault, A., Lozier, A., Wolfers, J., Flament, C., Tenza, D., Ricciardi-Castagnoli, P., Raposo, G., and Amigorena, S. (1998) Eradication of established murine tumors using a novel cell-free vaccine: dendritic cell derived exosomes. *Nat. Med.* **4,** 594–600
91. Steenblock, E. R., Wrzesinski, S. H., Flavell, R. A., and Fahmy, T. M. (2009) Antigen presentation on artificial acellular substrates: modular systems for flexible, adaptable immunotherapy. *Expert Opin. Biol. Ther* **9,** 451–464
92. Princiotta, M. F., Finzi, D., Qian, S.-B., Gibbs, J., Schuchmann, S., Buttgereit, F., Bennink, J. R., and Yewdell, J. W. (2003) Quantitating protein synthesis, degradation, and endogenous antigen processing. *Immunity* **18,** 343–354
93. Ring, A. M., Lin, J.-X., Feng, D., Mitra, S., Rickert, M., Bowman, G. R., Pande, V. S., Li, P., Moraga, I., Spolski, R., Ozkan, E., Leonard, W. J., and Garcia, K. C. (2012) Mechanistic and structural insight into the functional dichotomy between IL-2 and IL-15. *Nat. Immunol.* **13,** 1187–1195
94. Arneja, A., Johnson, H., Gabrovsek, L., Lauffenburger, D. A., and White, F. M. (2014) Qualitatively different T cell phenotypic responses to IL-2 versus IL-15 are unified by identical dependences on receptor signal strength and duration. *J. Immunol.* **192,** 123–135
95. Fehniger, T. A., Cooper, M. A., and Caligiuri, M. A. (2002) Interleukin-2 and interleukin-15: immunotherapy for cancer. *Cytokine Growth Factor Rev.* **13,** 169–183
96. Steenblock, E. R., and Fahmy, T. M. (2008) A comprehensive platform for *ex vivo* T-cell expansion based on biodegradable polymeric artificial antigen-presenting cells. *Mol. Ther.* **16,** 765–772
97. Almeida, J. P., Lin, A. Y., Figueroa, E. R., Foster, A. E., and Drezek, R. A. (2015) *In vivo* gold nanoparticle delivery of peptide vaccine induces anti-tumor immune response in prophylactic and therapeutic tumor models. *Small* **11,** 1453–1459
98. Håkerud, M., Selbo, P. K., Waeckerle-Men, Y., Contassot, E., Dziunycz, P., Kündig, T. M., Høgset, A., and Johansen, P. (2015) Photosensitisation facilitates cross-priming of adjuvant-free protein vaccines and stimulation of tumour-suppressing CD8 T cells. *J. Control. Release* **198,** 10–17
99. Hansen, J., Lindenstrøm, T., Lindberg-Levin, J., Aagaard, C., Andersen, P., and Agger, E. M. (2012) CAF05: cationic liposomes that incorporate synthetic cord factor and poly(I:C) induce CTL immunity and reduce tumor burden in mice. *Cancer Immunol. Immunother.* **61,** 893–903
100. Jin, J.-O., Zhang, W., Du, J.-Y., Wong, K.-W., Oda, T., and Yu, Q. (2014) Fucoidan can function as an adjuvant *in vivo* to enhance dendritic cell maturation and function and promote antigen-specific T cell immune responses. *PLoS ONE* **9,** e99396
101. Kobayashi, H., Dubois, S., Sato, N., Sabzevari, H., Sakai, Y., Waldmann, T. A., and Tagaya, Y. (2005) Role of trans-cellular IL-15 presentation in the activation of NK cell-mediated killing, which leads to enhanced tumor immunosurveillance. *Blood* **105,** 721–727
102. Giron-Michel, J., Giuliani, M., Fogli, M., Brouty-Boyé, D., Ferrini, S., Baychelier, F., Eid, P., Lebousse-Kerdilès, C., Durali, D., Biassoni, R., Charpentier, B., Vasquez, A., Chouaib, S., Caignard, A., Moretta, L., and Azzarone, B. (2005) Membrane-bound and soluble IL-15/IL-15R complexes display differential signaling and functions on human hematopoietic progenitors. *Blood* **106,** 2302–2310
103. Vámosi, G., Bodnár, A., Vereb, G., Jenei, A., Goldman, C. K., Langowski, J., Tóth, K., Mátyus, L., Szöllösi, J., Waldmann, T. A., and Damjanovich, S. (2004) IL-2 and IL-15 receptor α-subunits are coexpressed in a supramolecular receptor cluster in lipid rafts of T cells. *Proc. Natl. Acad. Sci. U.S.A.* **101,** 11082–11087
104. Stearns, R. C., Paulauskis, J. D., and Godleski, J. J. (2001) Endocytosis of ultrafine particles by A549 cells. *Am. J. Respir. Cell Mol. Biol.* **24,** 108–115
105. Zhao, Y., Sun, X., Zhang, G., Trewyn, B. G., Slowing, I. I., and Lin, V. S. (2011) Interaction of mesoporous silica nanoparticles with human red blood cell membranes: size and surface effects. *ACS Nano* **5,** 1366–1375
106. Hecht, T. T., Longo, D. L., and Matis, L. A. (1983) The relationship between immune interferon production and proliferation in antigen-specific, MHC-restricted T cell lines and clones. *J. Immunol.* **131,** 1049–1055
107. Sa, Q., Woodward, J., and Suzuki, Y. (2013) IL-2 Produced by CD8+ immune T cells can augment their IFN-γ production independently from their proliferation in the secondary response to an intracellular pathogen. *J. Immunol.* **190,** 2199–2207
108. Perica, K., Bieler, J. G., Schütz, C., Varela, J. C., Douglass, J., Skora, A., Chiu, Y. L., Oelke, M., Kinzler, K., Zhou, S., Vogelstein, B., and Schneck, J. P. (2015) Enrichment and Expansion with nanoscale artificial antigen presenting cells for adoptive immunotherapy. *ACS Nano* **9,** 6861–6871
109. Labowsky, M., Lowenthal, J., and Fahmy, T. M. (2015) An *in silico* analysis of nanoparticle/cell diffusive transfer: application to nano-artificial antigen-presenting cell:T-cell interaction. *Nanomedicine* **11,** 1019–1028
110. Labowsky, M., and Fahmy, T. M. (2013) Effect of cell surface deformation on synaptic factor accumulation during the early stages of T cell activation. *Chem. Eng. Sci.* **90,** 275–283